Analysis of Free Space Optic Link using Wavelength Diversity over Different Channel Models

Major Project Report

Submitted in partial fulfillment of the requirements

for the degree of

Master of Technology

in

Electronics and Communication Engineering

(Communication Engineering)

By

Bindiya Mishra

(14MECC02)

Electronics and Communication Engineering Branch

Electrical Engineering Department

Institute of Technology

Nirma University

Ahmedabad-382 481

May 2016

Analysis of Free Space Optic Link using Wavelength Diversity over Different Channel Models

Major Project Report

Submitted in partial fulfillment of the requirements

for the degree of

Master of Technology

in

Electronics and Communication Engineering

(Communication Engineering)

By

Bindiya Mishra
(14MECC02)

Under the guidance of

Prof. Dhaval G. Shah

Electronics and Communication Engineering Branch

Electrical Engineering Department

Institute of Technology

Nirma University

Ahemdabad-382 481

May 2016

Declaration

This is to certify that

1. The thesis comprises my orginal work towards the degree of Master of Technology in Communication Engineering at Nirma University and has not been submitted elsewhere for a degree.

2. Due acknowledgement has been made in the text to all other material used.

- Bindiya Mishra

Certificate

This is to certify that the Major Project entitled **"Analysis of Free Space Optic Link using Wavelength Diversity over Different Channel Models"** submitted by **Bindiya Mishra (14MECC02)**, towards the partial fulfilment of the requirements for the degree of Master of Technology in Communication Engineering of Nirma University, Ahmedabad is the record of work carried out by her under our supervision and guidance. In our opinion, the submitted work has reached a level required for being accepted for examination. The results embodied in this major project, to the best of our knowledge, haven't been submitted to any other university or institution for award of any degree or diploma.

Date:	Place: Ahmedabad
Guide	**Program Co-ordinator**
Prof. Dhaval G. Shah (Professor, EC)	**Dr. D. K. Kothari** (Professor, EC)
HOD	**Director**
Dr. P. N. Tekwani (Head of EE Department)	**Dr. P. N. Tekwani** (Director, IT-NU)

Acknowledgements

I would like to express my gratitude and sincere thanks to Dr. P. N. Tekwani Head of Electrical Engineering Department and Dr. D. K. Kothari Coordinator M.Tech Communication Engineering program for allowing me to undertake this thesis work and for his guidelines during the review process.

I am deeply indebted to my thesis supervisors Prof. Dhaval G. Shah for his constant support and motivation. I thank him for his esteem guidance which is the key factor to complete this thesis.

I wish to thank my friends of my class for their delightful company which kept me in good humor throughout the year.

Last, but not the least, no words are enough to acknowledge constant support and sacrifices of my family members because of whom I am able to complete the degree program successfully.

Bindiya Mishra
14MECC02

Abstract

In recent years, free space optic (FSO) communication has gained significant importance. It has many advantages over radio frequency (RF), such as high data rates, license-free operation, high security, and ease of deployment. The performance of FSO systems can be highly affected by fog and atmospheric turbulence. The turbulence effect is one of the biggest problems that face FSO systems, which degrades the overall system's performance. In this thesis, to mitigate the turbulence induced fading the information signal-carrying laser beam irradiance (intensity) is transmitted on more than one wavelength at same time by using wavelength diversity technique. As the refractive index variation will be different for different wavelengths, the fading is not same for different wavelength. The statistical analysis of the random irradiance fluctuations in FSO links is showed through the probability density function (PDF) of different channel model such as Lognormal, Gamma-Gamma, K channel and Exponentiated Weibull channel, from which we can measure the link performance in terms of outage probability and the bit error-rate (BER). The objective of this thesis is to examine the outage probability and BER performance of FSO systems with wavelength diversity over K-channel and Exponentiated Weibull channel. The source information was transmitted onto three carrier wavelengths 1550 nm, 1310 nm, and 850 nm. At receiver side, Optimal Combining (OC), Equal Gain Combining (EGC) and Selection Combining (SC) diversity schemes have been deployed to combine multiple carriers. The achieved results demonstrate that the wavelength diversity improve the performance of the FSO communication link, but at a significant escalation of the system's complication and budget.

Contents

List of Tables

List of Figures

Abbreviation

FSO .... Free Space Optics
RF .... Radio Frequency
PPM .... Pulse Position Modulation
DPSK .... Differential Phase Shift Keying
LED .... Light Emitting Diode
LD .... Laser Diode
APD .... Avalanche Photo Diode
AWGN .... Additive White Gaussian Noise
IM/DD .... Intensity Modulation / Direct Detection
MRC/OC .... Maximal Ratio Combining / Optimal Combining
EGC .... Equal Gain Combining
SC .... Selection Combining
PDF .... Probability Density Function
CDF .... Cumulative Distribution function
BER .... Bit Error Rate
SNR .... Signal to Noise Ratio

Chapter 1

Introduction

1.1 Free Space Optics Overview

Free Space Optics (FSO) is an optical communication technique that propagate the light in air, outer space, vacuum, or something similar to wirelessly transmit data for telecommunication. Currently, it is capable of up to 2.5 Gbps of data, video and voice communications through the air, and it allowing optical connectivity without requiring fiber optic cable. An FSO link consists of two optical transceivers accurately aligned to each other with a clear line-of-sight. It works in the range of few kilometers.

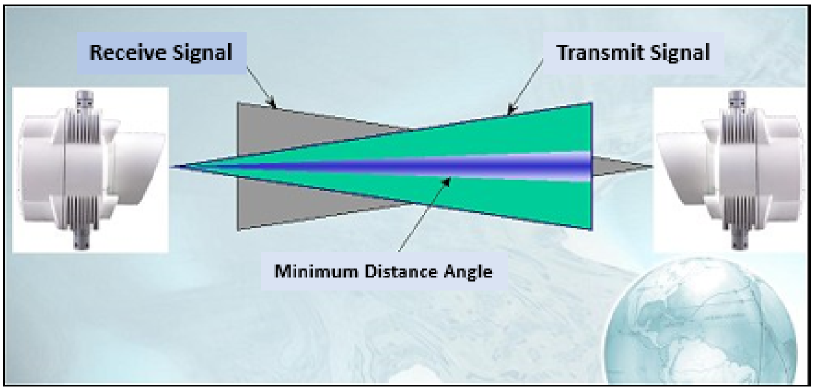

Figure 1.1: FSO system concept [3]

The earliest form of FSO is the photo phone of Alexander Graham Bell invented in 1880 [1]. In his experiment, Bell modulated the sun's radiation with voice signals and transmitted it over a distance of about 200 meters. However, the experiment did not go very well because of bad performance of the devices used and the nature of the sun's radiation. By the time of the discovery of laser in 1960, the problem of bad source of frequency carriers was solved.

1.2 Features of FSO

i **High modulation bandwidth:** The allowable bandwidth can be up to twenty percent of the carrier frequency. The usable range of carriers, whose frequency ranges from 1012-1016 Hz, could achieve up to 2000 THz data bandwidth. The usable frequency bandwidth in RF communication is comparatively lower by a factor of 105 [1].

ii **Narrow beam size:** Laser provides very narrow beam. It has a diffraction limit divergence of between 0.01 – 0.1 mrad. This shows that, the transmitted power is only concentrated within a very small area thus preventing an FSO link from potential interferes [1].

iii **Unlicensed spectrum:** Unlike RF communication, optical frequencies are free from all licenses and fees [1].

iv **Cheap:** The deployment cost of FSO link is lower than the RF with a comparable data rate. Based on a recent finding done by an FSO company in Canada, the cost per Mbps per month is about half that of RF based systems [2].

v **Quick to deploy and redeploy:** Time it takes for an FSO link to become fully operational starting from installation to link alignment could be as low as 4-5 hours. It can be taken down and redeployed to another location quite easily [1].

vi **Weather dependent:** FSO systems are also less affected by snow and rain compared to RF systems. But, it is highly affected by fog and atmospheric turbulence [1, 2].

1.3 Areas of Application

FSO can complement other technologies in making the huge bandwidth that resides in the optical fiber backbone available to end users. Most end users are within a short distance from the backbone network. This makes FSO very attractive as a data bridge between the backbone network and end users. It has been found suitable for use in the following areas:

i **Last mile access:** FSO can be used to bridge the bandwidth gap that exists between end users and the fiber optics backbone network.

ii **Optical fiber back up link:** It provide back up against loss of data or communication breakdowns in the event of damage or the lack of the main optical fiber link.

iii **Cellular communication back–haul:** It can be used to back haul traffic between base stations and switching centers in the new generation networks.

iv **Difficult terrain:** FSO is an attractive data bridge in the instances like a river, a street, rail tracks or where right of way is not available or very expensive to pursue [1, 2].

v **Military application:** FSO transmission is very secure as compared to other wireless technologies because the width of the transmitted beam is extremely narrow.

1.4 FSO Block Diagram

The block diagram of a FSO link is shown in Fig. 1.2. Like any other communication system, the FSO essentially contains three parts: transmitter, channel and receiver.

1.4.1 Transmitter

Here we consider the transmitter as a light source which has the task of sending light over the atmospheric channel. There are three types of light sources that are commonly used in FSO:

i **Light Emitting Diode (LED):** It can produce light in the 800-900 nm bands. It is very cheap and the most common light source. It has limited output powers (1-10 mW). LED has more frequency spreading than the other sources due to this the light tends to be unfocused.

ii **Laser:** Lasers have power outputs of 0.1-1 W and are more effective than light emitting diode. It has an optical cavity filled with light amplification material and a mirror at each side. The cavity lases an optical field travels on the two opposite sides. A small aperture in one of the mirrored sides allows some of the energy to escape as a radiated light.

iii **Laser Diode:** It is a semiconductor devices but it operate like lasers with reflecting etched substrates which act like small. LDs are small in size and very power efficient. It require more drive current than LEDs to generate more power. An LD produces optical power with a more focused than LEDs.

The wavelength chosen for FSO systems generally lies near 850 nm or 1550 nm. The shorter of the two wavelengths is cheaper and used for short distances. The 1550 nm is generally chosen for longer distances since it has a power allowance that is two orders of magnitude higher than at 850 nm. The cornea and lens are transparent to visible wavelengths, so, the power can reach the retina at the back of the eye. At

1550 nm retinal absorption is much lower since the power is absorbed mostly by the lens and cornea before it can reach the retina [4].

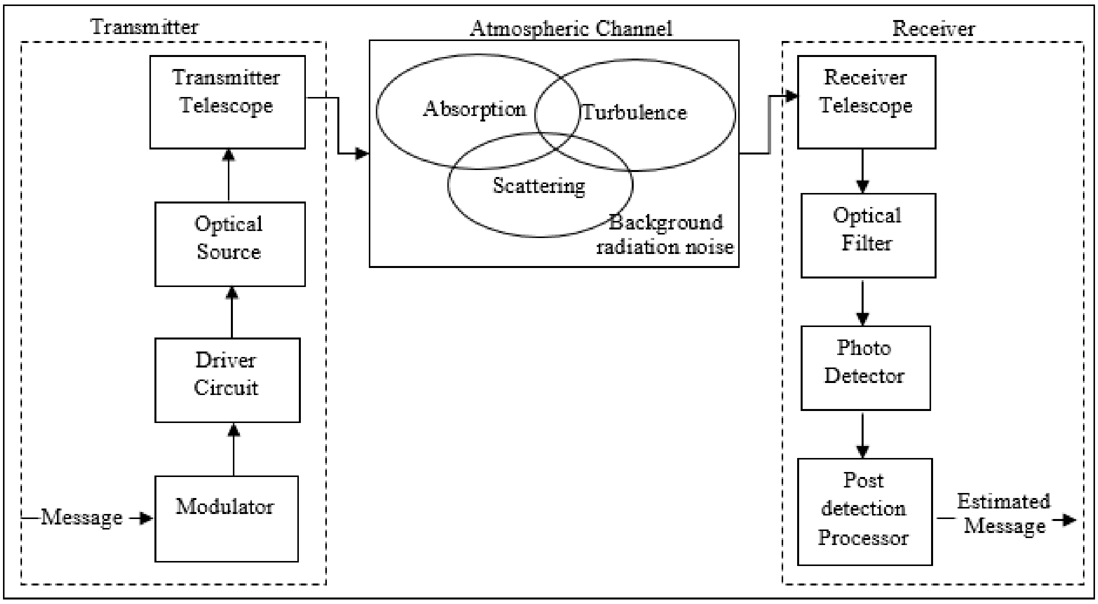

Figure 1.2: Block diagram of a terrestrial FSO link [1].

1.4.2 Receiver

The receiver recovers the transmitted data again from the incident optical path. The receiver part of FSO system consists:

i **Receiver telescope:** It collects and focuses incoming optical signal on to the photo detector. A large receiver telescope aperture is suitable as it collects multiple uncorrelated radiation and focuses their averages on the photo detector but the background noise increases too.

ii **An optical band pass filter:** It reduces the amount of background radiations.

iii **A photo detector:** The frequently used photo detectors are PIN Photo diodes and Avalanche Photodiodes (APD) that convert the incident optical signal into an electrical signal. APD is generally used in long distance optical communications because of the low received power levels. The performance of APD receivers is better than a PIN diode receiver, when the received power levels are very low.

iv **Post detection processor:** Where the amplification, filtering and signal processing necessary to guarantee a high reliability data recovered are carried out.

1.5 Modulation Schemes

The generally used modulation technique for FSO system is On-Off Keying (OOK) which offers bandwidth efficiency but lacks power efficiency. Pulse Position Modulation (PPM) achieves high power efficiency and improves system performance at the cost of reduced bandwidth efficiency compared with other modulation schemes. The optimal PPM order is high because a higher order modulation generates the higher peak power needed to overcome the weak average power. To overcome these problem, M-ary PPM has suggested as an appropriate modulation scheme for FSO systems [5]. Differential Phase Shift Keying (DPSK) modulation scheme is bandwidth efficient when coherent systems are employed in the logic that its performance is higher than Intensity Modulation/Direct Detection (IM/DD) systems against thermal noise. It also provides higher spectral efficiency. On the other hand, a coherent optical receiver is very complex than a simple direct detection receiver [6].

1.6 Different Receiving Techniques

The receiver detection process can be categorized into:

1.6.1 Direct Detection Receiver

This receiver detects the instantaneous intensity or power of the optical radiation incident on the photo detector. The output of the photo detector is proportional to the power of the incident radiation. Its operation is very simple and most suitable for intensity modulation optical systems [1, 2].

For optical wireless communication systems using intensity modulation, the output channel model depends on the intensity variation of the background light. In low background light case, the received signal can be modeled as a Poisson process with a rate of $\lambda_r(t) = \lambda_s(t) + \lambda_n(t)$, where λ_s is the number of signal photons per second and λ_n is the number of background noise photons per second. For $\lambda_n = 0$, the noise source is receiver preamplifier noise which is signal independent and is Gaussian. Infrared transceivers commonly operate in the presence of high levels of the ambient light originating from both natural and artificial sources. λ_n lies between 1011 and 1014 photons per second depending on the vicinity to a window. So, the photo-diode shot noise can accurately be modeled as additive white Gaussian noise (AWGN). Thus, the noise is usually modeled as Gaussian noise and signal independent.

To improve signal-to-noise ratio (SNR):

i **Increase the area of photodiode:** The area of photodiode A, must increase since the signal increases correspondingly with the photo diode area whereas the effective shot noise increases with $\sqrt{A}$. Therefore, the SNR can be enhanced at the cost of receiver speed since the photo diode capacitance also increases [7].

ii **Choose suitable filter:** The use of narrowband infrared filters instead of wideband filters [7].

1.6.2 Coherent Detection Receiver

The coherent receiver is based on the photo mixing phenomenon. The incoming optical field is mixed with another optical field on the surface of the photo detector. It can be separated into homodyne and heterodyne receivers. In homodyne receivers, the frequency of the local oscillator is exactly same as the incoming signal while in heterodyne detection, the incoming signal and the local oscillator frequencies are different.

In comparison to the RF coherent detection, the output of the local oscillator in an optical coherent detection is not required to have the same phase as the incoming radiation [1, 2].

1.7 FSO Channel Impairments

The performance of FSO system is controlled in the presence of channel losses induced by the atmospheric turbulence. These channel losses are:

1.7.1 Atmospheric Loss

An FSO systems is highly affected by different atmospheric conditions. Table 1.1 shows usual attenuation in different atmospheric conditions. Below the table, we discuss four main problem effects of the FSO system which are atmospheric attenuation, scintillation, window attenuation and beam divergence.

Table 1.1: Attenuation of FSO communication links [8].

Weather Condition	**Typical Attenuation (dB/km)**
Clear atmospheric conditions	0.2
Rain	40
Snow	100
Fog	120
Thick Fog	300
Dense Fog	480

i **Atmospheric Attenuation**

Atmospheric attenuation of FSO systems is commonly affected by fog but can also be dependent upon low clouds, rain, snow, dust and various combinations of each. During thick fog conditions when the visibility is even less than 40 m, attenuation can be more than 350 dB/km [9]. This shows that it could bound the availability of FSO link. In these cases, very high power lasers with special mitigation techniques help to improve the probabilities of link availability. Generally, 1550 nm lasers are ideal choice during the heavy attenuation because of their high transmitted power.

The influence of rain is not much pronounced like that fog as rain droplets are considerably larger (100 to 10,000 μm) than the wavelength used in FSO system. The choice of hybrid RF/FSO system improves the link performance especially for system operating at 10 GHz frequency and above.

Attenuation due to snow is more than rain but less than fog because the size of snow particles are between fog and rain. During heavy snow, the path of laser beam is blocked due to increase density of snowflakes in the propagation path.

ii **Scintillation**

Atmospheric scintillation can be defined as the intensity fluctuation of the received signal at the detector. Because of the intensity variation refractive index along the transmit path changes. These index changes cause the atmosphere to act like a series of small lenses that rebound portions of each light beam into and out of the transmit path as in Fig. 1.3. Scintillation can change during the course of a day. Overall, scintillation causes quick fluctuations of received power which increased the bit error rate of FSO performance [10].

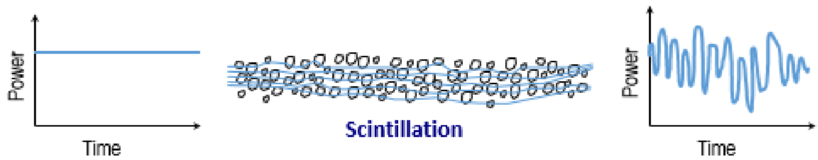

Figure 1.3: Illustration of scintillation effect on the received signal [8].

iii **Window Attenuation**

FSO system allow communication through windows without need for rooftop attached antennas. This is especially beneficial for connecting individual customers who may or may not have the access to a building's roof and also may have to pay for access to riser wiring of a building [10].

iv **Beam Divergence**

One of the main challenges with FSO systems is continuing transceiver alignment. FSO transceivers transmit highly directional and narrow beams of light each of 0.05–to 1.0 mrad divergence at the transmitter and usually spreads to roughly 5 cm to 1 m in diameter at a range of one kilometer. So, the system must be fixed powerfully to ensure sufficient amount of energy reaching at the receiver [10].

1.7.2 Noise

There are many causes of noise that must be considered when doing analysis on circuits. These are:

i **Shot Noise**

It occurs because of the randomness of photo electron creation. This randomness is due to the fact that, not every photon is going to be an electron-hole pair that gives to photo currents which affects the error probability [4].

ii **Background Noise**

The background noise enters into the receiver along with the signal. The way of reducing background noise is by blocking other sources of radiation by using a frequency selective filter in front of the receiver to only permit the signal to pass. The potential drawback of this method is that, it reduces the strength of the received signal [4].

iii **Thermal Noise**

Thermal noise is induced by the random fluctuations in the charge carriers of a resistive element. It is technically present in any of the semiconductor where thermally induced charge carriers can be present which even includes the photo detector itself, but it is only important in the resistor whose resistance is higher than the other sources. Both the PIN photo diode and APD are affected by thermal noise [4].

iv **Excess APD Noise**

The internal gain of APD rises the SNR value. However, due to the randomness of this amplification process excess noise created due to amplified shot noise but with a level more than if the primary shot noise is amplified alone. This excess noise is a function of the gain and ionization factor. The ionization factor is the ratio of the holes over electronics in the magnification region [11].

1.8 Mitigation Techniques in FSO Communication

Table 1.2: Challenges in optical wireless communications [1, 2, 8].

Challenges	**Causes**	**Effects**	**Mitigation Approach**
Safety	-Laser Radiation	-Damage to eyes and skin	-Power efficient modulation schemes: PPM -Use Class 1 lasers and 1550 nm wavelength
Noise	-Shot noise -Background noise -Thermal Noise -Excess Noise	-Low signal to noise ratio and high BER	-Optical filter
Turbulence	-Random refractive index variation	-Phase and intensity fluctuations (scintillation)	-Forward Error Correction -Reliable modulation -Diversity technique
Blocking	-Moving objects -Walls -Birds	-Temporary link outage	-Multiple Input Multiple Output -Hybrid FSO/RF
Weather Effects	-Fog, Rain, Gases, Smoke	-Attenuations, Scattering	-Transmit high power -Hybrid FSO/RF
Pointing Acquisition and Tracking	-Wind -Building sway	-Permanent link outage -Power loss	-Active tracking -Hybrid FSO/RF

1.9 Organization of the Thesis

The research work carried out during the course of time has been presented in total six chapters.

In Chapter 1 Introduction, basics of FSO, block diagram, different modulation techniques and detection techniques used for FSO has been presented. The problem and objective of the thesis is also stated in the first chapter.

In Chapter 2 Channel modelling, an overview of the key turbulence theory that will be used throughout this dissertation is explained. It also describes the laser beam propagation theory and various atmospheric channel model for different turbulence condition.

Chapter 3 Diversity includes the overview of diversity and different diversity techniques for mitigating the effect of turbulence in the atmosphere.

Chapter 4 K-Channel Model with Wavelength Diversity, in this chapter, wavelength diversity on the K channel model is described. A comparison of outage probability and average BER is also presented with the different atmospheric turbulence scenario and link length.

Chapter 5 Exponentiated Weibull Channel Model with Wavelength Diversity includes the overview of the Weibull distribution and Exponentiated Weibull distribution. It also describes the outage probability and average BER of the FSO system with the different link length.

Chapter 6 Conclusions and Future Work includes all the conclusions and scope for future work related to the free space optics.

Chapter 2

Channel Modelling

2.1 Introduction

The characteristics of wireless signal changes as it travels from the transmitter to the receiver. These characteristics depend upon the distance between transmitter and receiver, the path taken by the signal, the environment and other objects around the path. The profile of received signal can be obtained from that of the transmitted signal if we have a model of the medium between the two. This model of the medium is called **channel model** [12].

To design, implement and operate effective wireless optical communication systems, it is essential that the characteristics of the channel are well understood. Characterization of a wireless communication channel is achieved by its channel impulse response, which is then used to examine and combat the effects of channel distortions. The atmospheric channel has a very complex and dynamic environment that can affect the characteristics of the propagating optical beam, thus resulting in optical losses and turbulence induced amplitude and phase instability.

In this chapter we begin by the introduction of atmospheric turbulence, laser beam propagation theory and then discuss a statistical channel model that are based on changing value of the atmospheric turbulence.

2.2 Atmospheric Turbulence

All the models used to define the properties of the atmosphere on an optical traveling wave are based on the study of turbulence, which includes fluctuations in the velocity field of a viscous fluid [13]. These variations in the atmosphere are firstly due to temperature differences between the surface of the Earth and the atmosphere, and, to the differences in temperature and pressure within the atmospheric layers themselves, thus, producing pockets of air, also known as eddies, that cause the atmospheric turbulence. The different eddy sizes, i.e. the inertial range, responsible for the transfer of kinetic energy within the fluid, go from the outer scale Ł$_0$ to the inner scale l_0 of turbulence, where typical values of Ł$_0$ are between 10 and 20 m, while l_0 is usually around 1-5 mm. Such conditions comprise a range where wind energy is injected in the macroscale Ł$_0$, transferred through the inertial range and finally dissipated in the microscale l_0 [13]. This energy transfer causes unstable air masses, with temperature gradients, giving rise to local changes in the atmospheric refractive index and hence creating turbulence as optical wave propagates. Fig. 2.1 shows the Kolmogorov cascade model of turbulence as a function of spatial scale [14]. As turbulent eddies split, they become smaller and more uniform until all of their energy dissipates as heat.

The variations of the atmospheric refractive index n, which can be considered as locally homogeneous, can be mathematically expressed by

$$n(\overrightarrow{r}, t) = n_0 + n_1(\overrightarrow{r}, t) \tag{2.1}$$

where n_0 is the mean value of the refractive index; $n_1(\overrightarrow{r}, t)$ is a random variable with zero mean, signifying the changes caused by the atmospheric turbulence, and t shows the temporal dependence. According to Taylor frozen turbulence hypothesis [15], the turbulence is considered as stationary as the optical wave propagates, hence, the time dependence is usually dropped in (2.1).

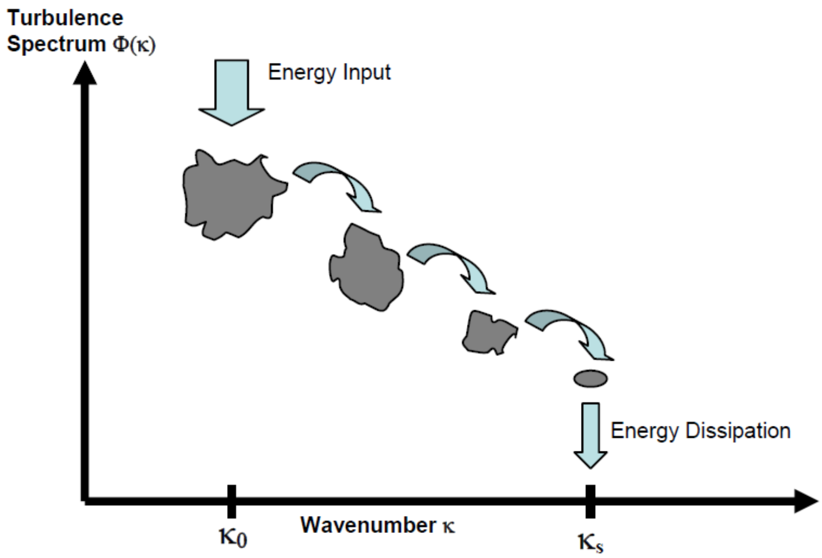

Figure 2.1: A pictorial description of the process of turbulent decay [14].

The statistical characterization of a locally homogeneous random field is generally done by its structure function, represented by

$$D_n(\overrightarrow{r_1}, \overrightarrow{r_2}) = \langle [n(\overrightarrow{r_1}) - n(\overrightarrow{r_2})]^2 \rangle \tag{2.2}$$

where there is no time dependence in the refractive index.

2.2.1 Refractive-index structure parameter

The atmospheric turbulence can be defined by the strength of the variations in the refractive index, characterized with the refractive index structure parameter C_n^2 in units of $m^{\frac{-2}{3}}$. Along the optical transmission path the value of C_n^2 has small variations for horizontal paths, while for gradient and vertical paths these variations become important [16]. When a vertical path is assumed, the performance of C_n^2 is conditioned by temperature changes along the different layers within the Earth's atmosphere, hence, the refractive index structure parameter turn out to be a function of the altitude above ground. The value of C_n^2 depends strongly on the hour of the day. It has a peak value at midday and local minima at sunrise and sunset. Provided that the time elapsed between the sunrise and sunset is different according to seasonal variations, the concept of temporal hour t_h has been introduced. The duration of a temporal hour is $\frac{1}{12^{th}}$ of the time between sunrise and sunset. In summer it is more than 60 min and in winter is lower, hence, it can be seen as a solar hour. The current t_h is obtained by subtracting the sunrise time from the local time, and dividing by the value of one t_h. Thus, in any day of the year $t_h = 00:00$ at sunrise, $t_h = 06:00$ at noon, and $t_h = 12:00$ at sunset. It should be noted that temporal hours are allowed to have negative time hours. In general, C_n^2 varies from $10^{-17}m^{\frac{-2}{3}}$ to $10^{-13}m^{\frac{-2}{3}}$ for weak to strong turbulence conditions, respectively [17].

2.2.2 Rytov approximation

A well-known method for analyzing the propagation of plane waves in weak turbulence is the Rytov method [13]. The Rytov solution for the intensity fluctuations of a plane wave, when the turbulence is appropriately weak, gives a variance for the log intensity variations of [18],

$$\sigma^2_{lnI_R} = \langle (lnI - \langle lnI \rangle)^2 \rangle = 1.23 C_n^2 k^{\frac{7}{6}} L^{\frac{11}{6}} \tag{2.3}$$

Here, R shows that this variance holds in the Rytov regime, when the turbulence is weak. Where the turbulence is not weak, it is still possible to refer to the Rytov variance, as calculated from (2.3), but this calculated variance will not same as the measured variance. It shows that the variance of the log normalized intensity variations $ln(\frac{I}{\langle I \rangle})$ is also equal to $\sigma^2_{lnI_R}$. Here, (2.3) demonstrates that as the strength of turbulence or the range L increase that the variance of the log intensity variations increases without limit. The Rytov method only predicts the correct variance provided

$\sigma^2_{lnI_R} < 0.3$. When this condition occur the turbulence is said to be weak. For weak turbulence $\langle (I/\langle I\rangle)^2 - 1\rangle \ll 1$. Strong turbulence condition may require $\sigma^2_{lnI_R}$ to be larger than 25.

Now other important parameter is the variance of the normalized intensity fluctuations, which is [18],

$$\sigma_I^2 = \frac{\langle I^2\rangle - \langle I\rangle^2}{\langle I\rangle^2} \tag{2.4}$$

For weak turbulence condition the Rytov variance can be expressed as [18],

$$\begin{aligned}\sigma^2_{lnI_R} &= \langle (ln(\frac{I}{\langle I\rangle}))^2\rangle = \langle (1 - \frac{I}{\langle I\rangle})^2\rangle \\ &= \frac{\langle I^2\rangle - \langle I\rangle^2}{\langle I\rangle^2}\end{aligned} \tag{2.5}$$

Therefore, in weak turbulence [18],

$$\sigma^2_{lnI_R} = \sigma_I^2 \tag{2.6}$$

We can say that, if the intensity variance is detected under the conditions of weak turbulence, it will be identical to the variance of the log intensity.

2.2.3 Extended Rytov theory

The Rytov approximation is valid only in weak irradiance fluctuations regime, and an extension of the theory is needed to address strong turbulence effects on optical traveling waves. As a wave propagates through the turbulent atmosphere its degree of transverse spatial coherence decreases [13, 19], this coherence loss is quantified by the spatial coherence radius [20]

$$\rho_0 = \begin{cases} (\frac{3}{1+\Theta+\Theta^2+\Lambda^2})^{\frac{1}{2}}(1.87C_n^2 L l_0^{\frac{-1}{3}})^{\frac{-1}{2}} & \rho_0 \ll l_0 \\ (\frac{8}{3(a+0.62\Lambda^{\frac{11}{6}})})^{\frac{3}{5}}(1.46C_n^2 L)^{\frac{-3}{5}} & l_0 \ll \rho_0 \ll L_0 \end{cases} \tag{2.7}$$

where a is a constant. It should be noted that Θ and Λ are dimensionless parameters associated with the Gaussian beam. The expression for ρ_0 in the limiting cases of plane wave $(\Lambda = 0, \Theta = 1)$, and spherical wave $(\Lambda = 0, \Theta = 0)$ can be deduced from (2.7).

Another parameter to measure the spatial coherence is the atmospheric coherence width $r_0 = 2.1\rho_0$, widely known as the Fried parameter. For the limiting case of a plane wave the Fried parameter is given by [20]

$$r_0 = (0.46C_n^2 k^2 L)^{\frac{-3}{5}} \tag{2.8}$$

Under the extended Rytov theory the refractive-index $n_1(\overrightarrow{r})$ in (2.1) can be seen as the result of the influence of two terms, i.e., the large-scale in-homogeneities $n_X(\overrightarrow{r}, t)$ and the small scale in-homogeneities $n_Y(\overrightarrow{r}, t)$. Thus, as the refractive index directly influences the turbulence power spectrum, an effective power spectral density for refractive index fluctuations can be expressed by [20]

$$\Phi_{ne}(k) = \Phi_n(k)G(k, l_0, L_0) = \Phi_n(k)[G_X(k, l_0, L_0) + G_Y(k, l_0)] \tag{2.9}$$

where G_X and G_Y are amplitude spatial filters modeling the large scale and small scale perturbations, respectively.

The effective atmospheric spectrum can be used instead of the classic spectrum to solve the statistical moments of a traveling optical field, thus, allowing to treat the effects of inner-scale size and outer-scale size of turbulence separately throughout the theory.

2.3 Laser Beam Propagation Theory

When optical wave propagates through the turbulent atmosphere, there are many effects that disturb the traveling wave front such as scintillation, which are occurred due to the random fluctuations of the traveling wave irradiance; beam wander, that is a continuous random movement of the beam centroid over the receiving aperture plane; angle-of-arrival fluctuations, which are associated with the dancing of the focused spot on the photo detector surface; and beam spreading that is the spreading beyond the pure diffraction limit of the beam radius.

A composite of several agitations suffered by an optical traveling wave front is shown in Fig. 2.2. Here, it is showed how small fluctuations in the atmospheric refractive index produce distortions in the wave front infuriating a random pattern, both in time and space, of self-interference of the beam at the points of the transverse receiver plane, and as a significance rapid variations of the received power appear [20].

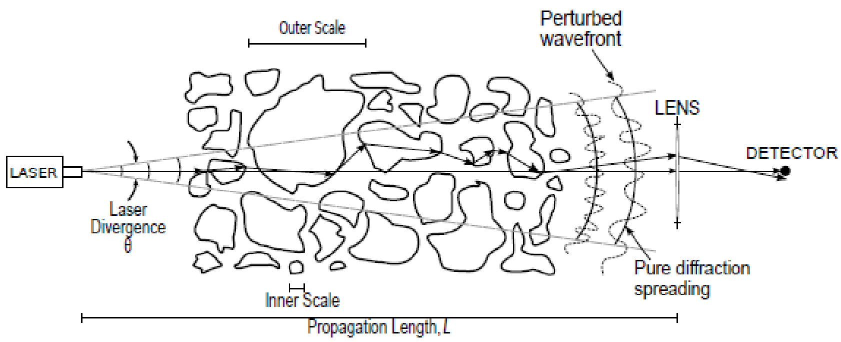

Figure 2.2: Laser beam propagation through the turbulent atmosphere [20].

The beams (dark lines) leaving the laser source are deflected as they travel through the largest air pockets, whose size defines the turbulence outer scale, arriving off axis instead of what is expected without turbulence, represented in Fig. 2.2 with the straight dashed arrow starting at laser and finishing at the receptor surface. Additionally, the turbulent atmosphere induces an extra spreading of the beam, i.e. the broadening of the beam size beyond of that expected due to pure diffraction, for the case of a laser beam. It is normal to refer as refractive effects to those caused by the outer scale size of turbulence, whereas, the inner scale sizes produce the diffractive effects. As the rays may also be interpreted as the wave vector for the traveling wave front, the variations in the angle respect to the optical axis at the receiver represent the concept of angle-of-arrival fluctuations. Moreover, this bouncing of the optical wave front as it propagates through the atmosphere is also responsible for the beam wander effect as the centroid of the laser beam is displaced randomly at the receiver plane. Furthermore, fog, rain, snow, haze, and generally any floating particle can cause extinction of the signal carrying laser beam intensity. In a worst case scenario the intensity attenuation can be strong enough to cause link outages, leading to a high bit error-rate that inevitably decreases the overall system performance and limits the maximum length for the optical link.

Following this we consider some details of an atmospheric turbulence condition and then provide a section in which the statistical channel models are discussed.

2.4 Classic FSO Fading Models

To describe the statistical behavior of the atmospheric channel many models have been suggested. The most widely accepted channel models are the Log-Normal (LN) and the Gamma-Gamma (GG) models. We consider an FSO system using IM/DD (Intensity Modulation/ Direct Detection) with OOK, which is extensively deployed in systems. The laser beams transmit along a horizontal path through an offered turbulence channel with additive white Gaussian noise (AWGN). The received signal is given by

$$y = hx + n \tag{2.10}$$

where x is the binary transferred signal, $h = \eta I$ is the channel coefficient considered to be constant over a large number of transferred bits, η is the effective photo-current conversion ratio of the receiver, I is the normalized irradiance received at the receiver, and n is AWGN with variance $\sigma_n^2 = \frac{N_0}{2}$. Since OOK modulation system is used, x is either 0 or 1.

In this section, classic FSO fading models have been proposed to model the unsystematic phenomena of turbulence. These include the Log-normal and Gamma-Gamma channel model.

2.4.1 Lognormal Channel Model

Lognormal distribution is mostly used model for the probability density function (PDF) of the random irradiance over atmospheric channels. This model is only valid for weak turbulence conditions and for distances less than 100 meter. Considering lognormal model, the pdf of the received irradiance I is given as $f(I)$ [21];

$$f(I) = \frac{1}{\sqrt{2\pi\sigma_i^2 I}} exp\left[- \frac{(ln(I) - m_i)^2}{2\sigma_i^2} \right], I \geq 0 \tag{2.11}$$

where m_i is the mean value and σ_i shows the standard deviation of irradiance, the scintillation index σ_{SI}^2 describe as a function of variance σ_i^2 is $\sigma_{SI}^2 = exp[\sigma_i^2] - 1$. Therefore $\sigma_i^2 = ln(\sigma_{SI}^2 + 1)$.

2.4.2 Gamma-Gamma Channel Model

The Gamma-Gamma distribution is used to model the two independent contributions of the small-scale and large-scale of turbulence, assuming each of them is governed by a Gamma process. The GG distribution is then given by [22]:

$$f(I) = \frac{2(\alpha\beta)^{\frac{(\alpha+\beta)}{2}}}{\Gamma(\alpha)\Gamma(\beta)} I^{\frac{(\alpha+\beta)}{2}-1} K_{\alpha-\beta}(2\sqrt{\alpha\beta I}), I \geq 0 \tag{2.12}$$

Where $K_\alpha(.)$ is the modified Bessel function of second order, α and β are the scattering parameters of environment. These parameters are directly related to atmospheric conditions according to

$$\alpha = \left[exp\left(\frac{0.49\chi^2}{(1 + 0.18d^2 + 0.56\chi^{\frac{12}{5}})^{\frac{7}{6}}} \right) - 1 \right]^{-1}$$

$$\beta = \left[exp\left(\frac{0.51\chi^2}{(1 + 0.9d^2 + 0.62d^2\chi^{\frac{12}{5}})^{\frac{5}{6}}} \right) - 1 \right]^{-1}$$

where $\chi^2 = 0.5C_n^2 k^{\frac{7}{6}} L^{\frac{11}{6}}$ and $d = \left(\frac{kD^2}{4L}\right)^{\frac{1}{2}}$, $k = \frac{2\pi}{\lambda}$ is the optical wave number, λ is the wavelength and D is the diameter of the receiver collecting lens aperture. C_n^2 gives the value of refractive index structure parameter.

Chapter 3

Diversity

3.1 Introduction

In wireless communication the term diversity refers to a method for improving the reliability of a message signal by using two or more than two communication channels with different characteristics. Multiple forms of the same signal may be transmitted and/or received and combined in the receiver.

3.2 Types of Diversity

Small scale fades are characterized by deep and rapid amplitude fluctuations which occur as mobile moves over distances of just a few wavelengths. For narrow-band signals, this typically results in a Rayleigh faded envelope. In order to prevent the deep fades from occurring, microscopic diversity techniques can exploit the rapidly changing signal.

Large scale fading, caused due to shadowing, can be combated using macroscopic diversity wherein the distances of consideration are of the order of the distances between two base stations.

3.3 Diversity Schemes

To combat the effect of fading, different diversity techniques are used. The following classes of diversity schemes can be identified:

i Time diversity

ii Frequency diversity

iii Wavelength diversity

iv Space diversity

v Polarization diversity

vi Multiuser diversity

3.3.1 Time Diversity

The information signal is transmitted repeatedly in time at regular intervals. The separation between the transmit times should be greater than the coherence time T_c. The time interval depends on the fading rate, and increases with the decrease in the rate of fading.

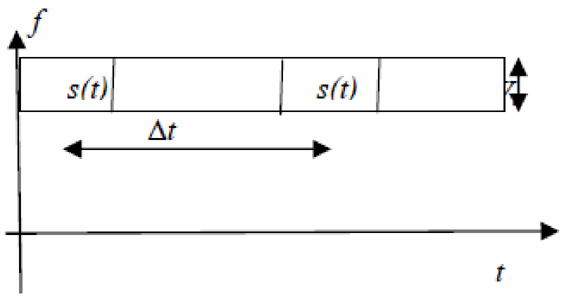

Figure 3.1: Time Diversity [23].

3.3.2 Frequency Diversity

The same information signal is transmitted on different carriers, the frequency separation between them being at least the coherence bandwidth.

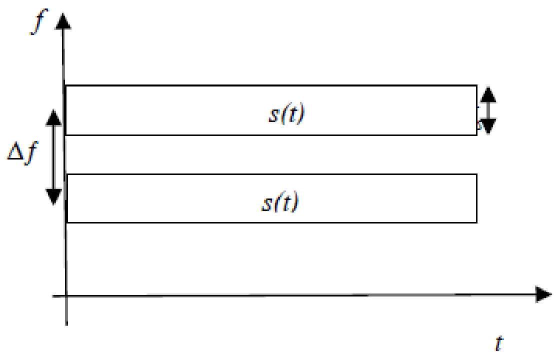

Figure 3.2: Frequency Diversity [23].

3.3.3 Wavelength Diversity

When wavelength diversity is employed, system uses a composite transmitter and the signal is transmitted at the same time at different wavelengths towards a number of receivers, each of which detects the signal at a specific wavelength only.

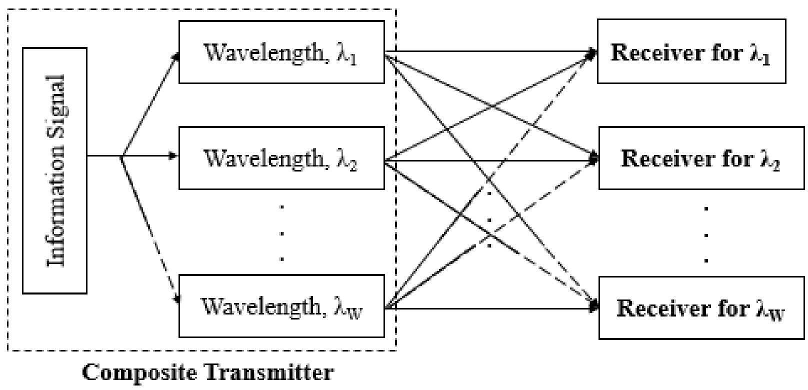

Figure 3.3: Wavelength Diversity.

3.3.4 Space/Spatial Diversity

In Space diversity, there are multiple receiving antennas placed at different spatial locations, resulting in different (possibly independent) received signals.

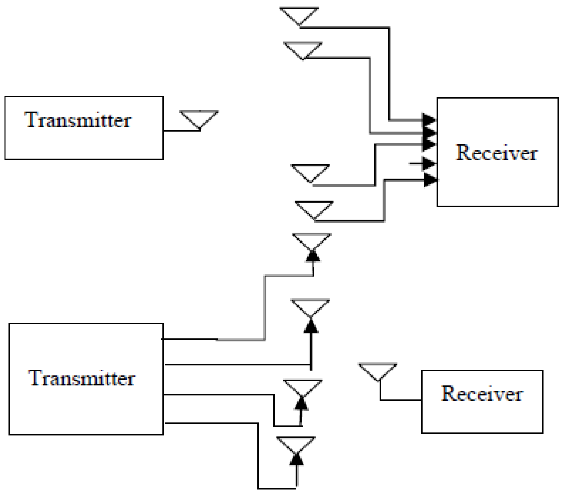

Figure 3.4: Space Diversity: 1 T_X–N R_X and N T_X-1 R_X Antennas [23].

3.3.5 Polarization Diversity

Here, the electric and magnetic fields of the signal carrying the information are modified and many such signals are used to send the same information. Thus orthogonal type of polarization is obtained. It enables detection of smaller radar cross section targets, and avoids the physical, mathematical, and engineering challenges of time of arrival coherent combining. The advantage of polarization diversity over spatial diversity is that diversity gains are possible with collocated antennas.

3.3.6 Multiuser Diversity

Multiuser diversity is obtained by opportunistic user scheduling at either the transmitter or the receiver. Opportunistic user scheduling is as follows: at any given time, the transmitter selects the best user among candidate receivers according to the qualities of each channel between the transmitter and each receiver. A receiver must feedback the channel quality information to the transmitter using limited levels of resolution, in order for the transmitter to implement Multiuser diversity.

3.4 Diversity Combining Techniques

It is necessary to combine the uncorrelated faded signals which were obtained from the diversity branches to get proper performance. The combining system should be in such a manner that improves the performance of the communication system like the signal-to-noise ratio (SNR) or the power of received signal. Mainly, the combining should be applied in reception; however it is also possible to apply in transmission. Following are the various receiver diversity combining methods:

3.4.1 Maximal Ratio Combining (MRC)/ Optimal Combining (OC):

The MRC technique needs summing circuits, weighting and co-phasing. Signals from different diversity branches are co-phased and weighted before combining. The weights have to be chosen as proportional to the respective signals level for maximizing combined carrier-to-noise ratio (CNR). The applied weighting to the diversity branches has to be adjusted according to the SNR value. For maximizing the SNR and minimizing the error probability at the output, signal of dth diversity branch is weighted before making sum with others by a factor of $\frac{c'_d}{\sigma^2_{n,d}}$ [24]. Here $\sigma^2_{n,d}$ is noise variance of d^{th} diversity branch and c'_d complex conjugate of channel gain. As a result, the phase-shifts are compensated in the diversity channels and the signals coming from strong diversity branches which has low level noise are weighted more comparing to the signals from the weak branches with high level of noise. The term $\sigma^2_{n,d}$ in weighting can be neglected conditioning that $\sigma^2_{n,d}$ has equal value for all d. Then the realization of the combiner needs the estimation of gains in complex channel and it does not need any estimation of the noise power.

The MRC is a commonly used combining method to improve performance in a noise limited communication systems where the AWGN and the fading are independent amongst the diversity branches. This is the best combining process which achieves the best performance improvement on comparing to other methods.

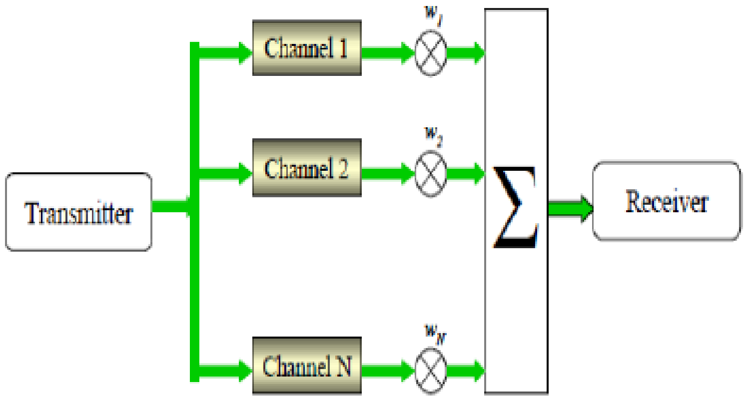

Figure 3.5: Maximal-Ratio Combining (MRC) [24].

3.4.2 Equal Gain Combining (EGC):

The EGC method is similar to MRC with an exception to omit the weighting circuits. The performance improvement is little bit lower in EGC than MRC because there is a chance to combine the incoming signals with interference and noise, with the signals in high quality which are interference and noise free.

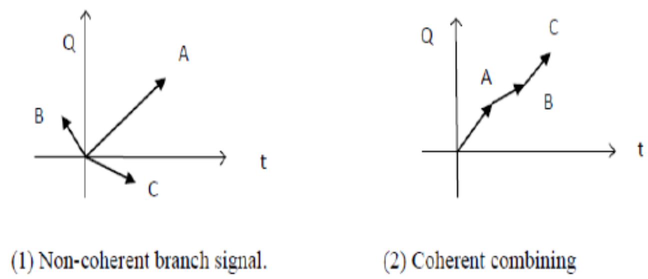

Figure 3.6: Equal Gain Combining [24].

The normal procedure of EGC is coherently combined the individual signal branch but it non-coherently combine some noise components according to following Fig. 3.6.

MRC is the most ideal diversity combining but the scheme requires very expensive design at receiver circuit to adjust the gain in every diversity branch. It needs an appropriate tracking for the complex fading, which is very difficult to achieve practically. However, by using a simple phase lock summing circuit, it is very easy to implement an equal gain combining.

The EGC can employ in reception of diversity with coherent modulation. The envelope gains of diversity channels are neglected in EGC method and the diversity branches are combined here with equal weights but conjugate phase. The structure of the EGC is as following since there is no envelope gain estimation of the channel.

3.4.3 Selection Combining (SC):

The MRC and EGC methods are not suitable for very high frequency (VHF), ultra high frequency (UHF) or mobile radio applications because realization of a co-phasing circuit with precise and stable tracking performance is not easy in a frequently changing, multipath fading and random-phase environment. SC method uses simple implementation procedure and is more suitable comparing to MRC and EGC in mobile radio application.

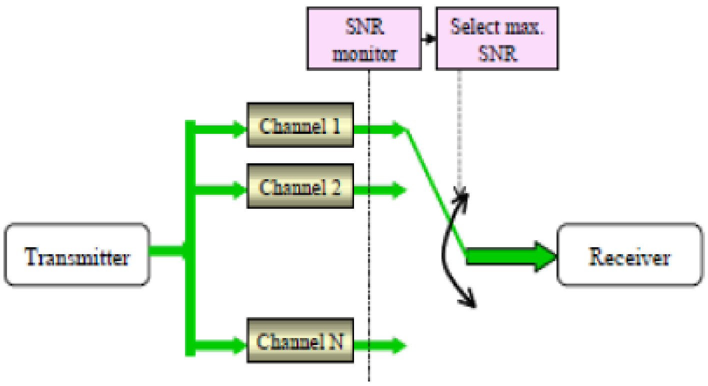

Figure 3.7: Selection Combining [24].

In SC technique, the diversity branch which has the highest signal level has to be selected. Refer the Fig. 3.7, the general form of selection combining is to monitor all the diversity branches and select the one which has the highest SNR. However, computing highest SNR is quite difficult because the system has to select it in a very short time. But selecting the branch with the highest SNR is similar to select the branch with highest received power when average power of noise is same on each branch. Therefore, it is practical to select the branch which has largest signal composition, noise and interference. The performance improvement achieved by the selection combining is just little lower than performance improved achieved by an ideal MRC and EGC. As a result the SC is the most used diversity scheme in wireless communication. If there is an availability of feedback information about channel state of the diversity branch the selection combining also can be used in transmission.

Different types of diversity schemes have their own merits and demerits. So in different environment different diversity schemes are selected. Combining schemes is also application and environment dependent.

3.5 Diversity technique for mitigating the turbulence effect in FSO system

Diversity technique for mitigating the effect of turbulence in the atmosphere can operate on time, frequency, wavelength and space. In this case, instead of single large aperture, an array of smaller receiver aperture is used so that multiple copies of the signal that are mutually uncorrelated and can be transmitted either in time or frequency or wavelength or space. This will improve the link availability and BER performance of the FSO system. It also limits the need of active tracking due to laser misalignment. By using diversity technique in FSO system, scintillation index was drastically improved. The gain due to diversity is more pronounced at high turbulence level than at lower values. In case of receiver diversity (SIMO- single input multiple output), diversity gain is achieved by averaging over multiple independent signal paths. The signals can be combined at the receiver using selection combining (SC) or equal gain combining (EGC) or maximal ratio combining (MRC). SC is simpler as compared to other two, but gain in this case is low. The gain achieved through MRC is slightly higher than EGC, but at the expense of complexity and cost. Therefore, implementation of EGC is preferred over MRC due to its simplicity and comparable performance.

For transmit diversity (MISO- multiple input single output), special space time codes such as optical Alamouti code is used. This code is designed only for two transmit antenna but can be extended to more number of antennas. The performance of optical MIMO (multiple input multiple output) and RF MIMO systems are almost equivalent. It increases the channel capacity of the system almost linearly with the number of transmitting antenna.

Chapter 4

K-Channel Model with Wavelength Diversity

4.1 Introduction

It is well known that the performance of free space optical systems strongly depend on the atmospheric conditions in the area of the established link. In order to combat the atmospheric turbulence effect on the operation of FSO links, apply diversity methods. V. Xarcha, A. N. Stassinakis, et.al [25] have applied wavelength diversity over log-normal channel and calculated the outage probability and average BER of the FSO system for low turbulence condition. In [26], Hector E. Nistazakis and George S. Tombras have applied wavelength and time diversity over Gamma- Gamma channel and evaluated performance of FSO system in terms of average BER and outage probability for moderate turbulence condition. In this chapter, I have considered the FSO system with wavelength diversity over K turbulence channel and evaluate their reliability and performance by the achieved outage probability and average BER for strong turbulence condition.

4.2 K-Channel Model

K-Channel model is used in strong turbulence condition. Here, scintillation index is nearly 1 and the value of log intensity variance is between 3 and 4. This channel model can be considered as a product of Exponential model and Gamma model. This model provides excellent agreement between theoretical and experimental values. PDF for K channel model is [27]:

$$f(I) = \frac{2(\alpha)^{\frac{(\alpha+1)}{2}}}{\Gamma(\alpha)} I^{\frac{(\alpha-1)}{2}-1} K_{\alpha-1}(2\sqrt{\alpha I}), I \geq 0 \tag{4.1}$$

where α is the channel parameter related to the effective number of discrete scatters, I is the normalized irradiance, $\Gamma(.)$ is the well-known Gamma function and $K_v(.)$ is the v^{th} order modified Bessel function of the second kind. When $\alpha \to \infty$, (4.1) approaches the negative exponential (NE) distribution.

4.3 FSO system with Wavelength Diversity

In FSO communication system, the wavelength diversity can be modeled as a system that uses a composite transmitter, transmitting a signal at different wavelengths at the same time instant towards all the receivers and each receiver will detect signal at a particular wavelength. Suppose that an FSO system comprises of W different pair of transmitter and receivers and the information signal is pass on all together by the W transmitters at W different wavelengths. Then, each w^{th} of these copies of the signal, $w = 1, ..., W$, will be detected only by w^{th} receiver. For a few kilometers link distances and aperture separation of the photo detectors is of order of centimeters, these W receivers will be practically uncorrelated [28]. We consider the w^{th} laser beam as it propagates along a horizontal path through turbulence channel with additive white Gaussian noise (AWGN). The channel is assumed to be memory less, stationary and ergodic, with independent and identically distributed (i.i.d.) intensity fast fading statistics, intensity modulation/direct detection (IM/DD) with

On–Off Keying (OOK) modulation. In this case, the statistical channel model can be considered as [25]:

$$y_w = h_w x + n = \eta_w x I_w + n, w = 1, ..., W \tag{4.2}$$

where y_w is the output signal of each of the W receivers, $h_w = \eta_w I_w$ is instantaneous intensity gain, η_w is effective photo current conversion ratio of each receiver, I_w is the normalized irradiance arrived in each receiver and x is the modulated signal with binary values '0' or '1', and n represents the AWGN with zero mean and variance equal to $\frac{N_0}{2}$.

For K channel model the PDF of the normalized irradiance with wavelength diversity is;

$$f_{I_w}(I_w) = \frac{2(\alpha_w)^{\frac{(\alpha_w+1)}{2}}}{\Gamma(\alpha_w)} I_w^{\frac{(\alpha_w-1)}{2}-1} K_{\alpha_w-1}(2\sqrt{\alpha_w I_w}), I_w \geq 0 \tag{4.3}$$

where α_w and I_w are the channel parameter related to the effective number of discrete scatters and normalized irradiance, respectively with w^{th} wavelength. $K_v(.)$ in terms of the Meijer G-function can be written as [29];

$$K_v(.) = \frac{1}{2} G^{2\,0}_{0\,2}\left(\left. \begin{matrix} - \\ \frac{v}{2}, \frac{-v}{2} \end{matrix} \right| \frac{x^2}{4} \right) \tag{4.4}$$

By using the above conversion the CDF of I can be easily derived by

$$F_{I_w}(I_w) = \int_0^\infty f_{I_w}(I_w) dI_w \tag{4.5}$$

$$F_{I_w}(I_w) = \int_0^\infty \frac{(\alpha_w I_w)^{\frac{\alpha_w+1}{2}}}{\Gamma(\alpha_w)} I_w^{0-1} G^{2\,0}_{0\,2}\left(\left. \begin{matrix} - \\ \frac{\alpha_w-1}{2}, \frac{-(\alpha_w-1)}{2} \end{matrix} \right| \alpha_w I_w \right) dI_w \tag{4.6}$$

Now using [29, eqn. (26)] and [30, eqn. (07.34.16.0001.01)], (4.6) can be written as

$$F_{I_w}(I_w) = \frac{1}{\Gamma(\alpha_w)} G_{1\ 3}^{2\ 1} \left({}_{\alpha_w,1,0}^{1} \middle| \alpha_w I_w \right) dI_w \tag{4.7}$$

The scintillation index (*SI*) can be calculated by using [36];

$$SI \triangleq \frac{E[I_w^2] - E^2[I_w]}{E^2[I_w]} = \frac{\alpha_w + 2}{\alpha_w} \tag{4.8}$$

where $E[.]$ gives the expected value of the enclosed. Since SI depends on the parameter α_w, it can be see that the turbulence is stronger for lower values of α_w and gets weaker as α_w increases. The scintillation strength can also described by the Rytov variance and spatial coherence radius [13, 14],[20]. The instantaneous electrical SNR can be defined as $\gamma_w = \frac{(\eta_w I_w)^2}{N_0}$ and the average electrical SNR is defined as, $\mu_w = \frac{(\eta_w E[I_w])^2}{N_0}$ [25, 26]. Here, $E[I_w] = 1$ since I_w is normalized. After a power transformation of the random variable I_w, the PDF for the instantaneous electrical SNR, γ_w can be derived as,

$$f_{\gamma_w}(\gamma_w) = \frac{\alpha_w^{\frac{(\alpha_w+1)}{2}} \gamma_w^{\frac{a_w-3}{4}}}{\Gamma(\alpha_w) \mu_w^{\frac{a_w+1}{4}}} K_{\alpha_w - 1}\left(2\sqrt{\alpha_w \sqrt{\frac{\gamma_w}{\mu_w}}} \right), \gamma_w \geq 0 \tag{4.9}$$

And the corresponding CDF of the instantaneous electrical SNR γ_w is;

$$F_{\gamma_w}(\gamma_w) = \frac{1}{\Gamma(\alpha_w)} G_{1\ 3}^{2\ 1} \left({}_{\alpha_w,1,0}^{1} \middle| \alpha_w \sqrt{\frac{\gamma_w}{\mu_w}} \right) dI_w \tag{4.10}$$

Thus, from mathematical expressions (4.9) and (4.10) it is clear that both PDF and CDF of the K channel strongly depends on the different physical parameters of the optical link.

4.4 The outage probability of the system

The outage probability is the point after which receiver will not receive any meaningful signal. Beyond this point noise will dominant over signal. This provides probability at which the spontaneous SNR falls below the threshold SNR, γ_{th} which is related to the receiver's input sensitivity limit [25]-[27]. Following the above stated definition of the outage probability and using (4.8), closed form expression is derived for the assessment of the outage performance of the FSO communication system with wavelength diversity, using optimal combining (OC) and selection combining (SC) method at the receiver end.

4.4.1 Optimal Combining (OC)

The outage probability, $P_{out,w}$ of each optical communication channel of the L different wavelength channels is given by,

$$P_{out,w} = P_r(\gamma_w \leq \gamma_{th,w}) = F_{\gamma_w}(\gamma_{th,w}), w = 1, ..., W \tag{4.11}$$

And using (4.10):

$$F_{\gamma_w}(\gamma_w) = \frac{1}{\Gamma(\alpha_w)} G^{2\ 1}_{1\ 3}\left({}^{1}_{\alpha_w,1,0} \middle| \alpha_w \sqrt{\frac{\gamma_{th,w}}{\mu_w}} \right) \tag{4.12}$$

Assuming that $P_{out,w}$ is autonomous for different wavelengths. Now the FSO communication system's total outage probability $P^{OC}_{out,W}$ will then relate to outage probability of all the W links, i.e.:

$$P^{OC}_{out,W} = \prod_{w=1}^{W} P_{out,w} = \prod_{w=1}^{W} P_r(\gamma_w \leq \gamma_{th,w}) = \prod_{w=1}^{W} F_{\gamma_w}(\gamma_{th,w}) \tag{4.13}$$

And using again (4.10):

$$P^{OC}_{out,W} = \prod_{w=1}^{W} \left[\frac{1}{\Gamma(\alpha_w)} G^{\,2\,1}_{\,1\,3} \left({}^{\;\;1}_{\alpha_w,1,0} \middle| \alpha_w \sqrt{\frac{\gamma_{th,w}}{\mu_w}} \right) \right] \tag{4.14}$$

The numerical result of (4.14) is shown in Fig. 4.1.

4.4.2 Selection Combining (SC)

Let γ_{th} is the threshold value of the SNR. If there are W links (i.e., W transmitters and W receivers), the probability at which the signal to noise ratio of all the links are lower the threshold γ_{th} is

$$P_{out,w} = P(max\{\gamma_1, \gamma_2, ..., \gamma_w\}) \tag{4.15}$$

Now,

$$P_{out,w} = P_r(\gamma \leq \gamma_{th,w}) = F_\gamma(\gamma_{th,w}) = \frac{1}{\Gamma(\alpha_w)} G^{\,2\,1}_{\,1\,3} \left({}^{\;\;1}_{\alpha_w,1,0} \middle| \alpha_w \sqrt{\frac{\gamma_{th,w}}{\mu_w}} \right) \tag{4.16}$$

Assuming that $P_{out,w}$ is autonomous for the different wavelength channels. Now, total outage probability $P^{SC}_{out,W}$ of the FSO system which is taken into account will correspond to the outage probabilities of all the channels with different wavelengths.

$$P^{SC}_{out,W} = \left[\frac{1}{\Gamma(\alpha)} G^{\,2\,1}_{\,1\,3} \left({}^{\;1}_{\alpha,1,0} \middle| \alpha \sqrt{\frac{\gamma_{th}}{\mu}} \right) \right]^W \tag{4.17}$$

The numerical result of (4.17) is shown in Fig. 4.2.

In Fig. 4.1 and Fig. 4.2 we have compared the outage probability performance of the system for link length $L_1 = 2km$ and $L_2 = 3km$ using OC and SC method at the receiving end, respectively. We consider receiver aperture diameter, $D = 0.01m$ and assume three wavelengths $\lambda_1 = 1550nm, \lambda_2 = 1310nm$ and $\lambda_3 = 850nm$ and for the strong atmospheric turbulence condition $C_n^2 = 2 \times 10^{-13} m^{\frac{-2}{3}}$. And also assume that the average electrical SNR and the sensitivity limits are the same for all the W receivers, i.e., $\mu_1 = \mu_2 = ... = \mu_W = \mu$ and $\gamma_{th,1} = \gamma_{th,2} = ... = \gamma_{th,W} = \gamma_{th}$.

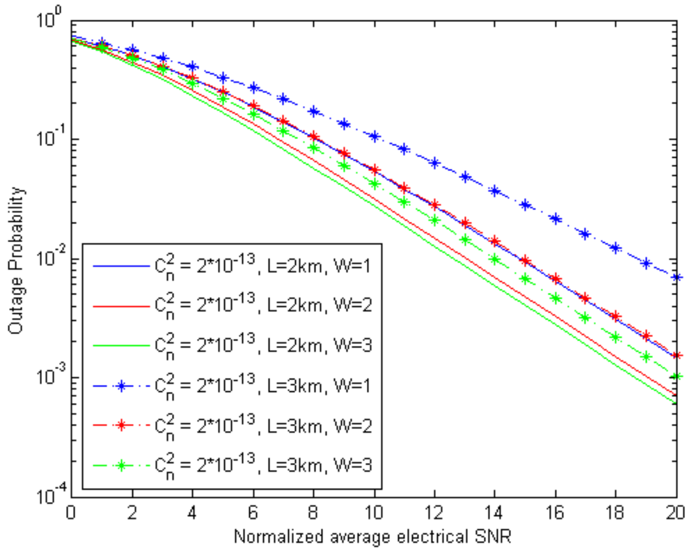

Figure 4.1: Outage probability of the FSO systems with wavelength diversity, versus the normalized average electrical SNR for OC.

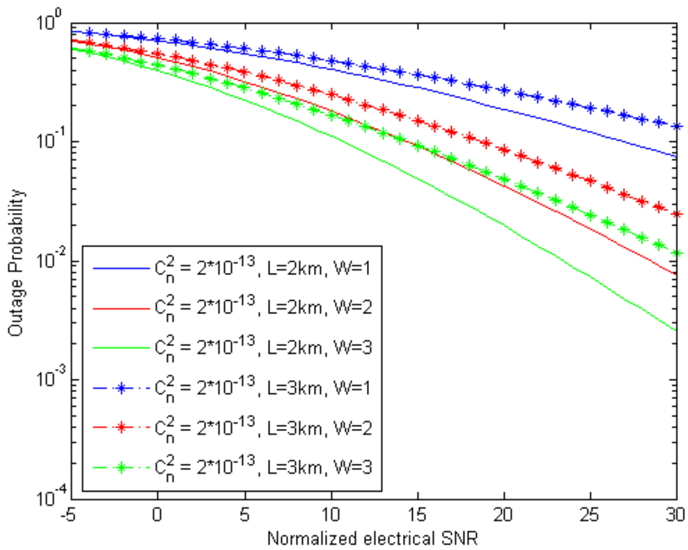

Figure 4.2: Outage probability of the FSO systems with wavelength diversity, versus the normalized average electrical SNR for SC.

It is clearly evident from these figures, that the outage probability of the FSO links using wavelength is getting much smaller as the number of elements (W) of the different wavelength channels are increasing. It is expected as each wavelength suffers different attenuation under atmospheric conditions. The accessibility of an FSO system can be defined by its outage probability, $P_{out,W}$.

4.5 The Average BER of the System

The average bit error rate is an important metric for the reliability of a communication system. For the considered FSO system with IM/DD and OOK, the estimation, of BER, P_e, in the presence of AWGN can be done through the expression:

$$P_e = P(1)P(e \mid 1) + P(0)P(e \mid 0) \tag{4.18}$$

where $P(1)$ and $P(0)$ are the probabilities of sending 1 and 0 bits, respectively, and $P(e \mid 1)$ and $P(e \mid 0)$ represent the conditional bit error probabilities when the transmitted bit is 1 and 0. Then assuming that the condition is symmetric, i.e. $P(1) = P(0) = 0.5$, and $P(e \mid 1) = P(e \mid 0)$, the estimation of BER for SISO link, as a function of I, is given as:

$$P(I) = P(e \mid 1, I) + P(e \mid 0, I) = Q\left(\frac{\eta I}{\sqrt{2N_0}}\right) = Q\left(\sqrt{\frac{\gamma}{2}}\right) \tag{4.19}$$

where $Q(.)$ is the Gaussian Q-function defined as $Q(x) = \left(\frac{1}{\sqrt{2N_0}}\right) \int_x^\infty exp\left(\frac{t^2}{2}\right) dt$ and this is also related to the complimentary error function $erfc(.)$ by $erfc(x) = 2Q(\sqrt{2}x)$.

The average BER for SISO link of the FSO system, P_{av} is obtained by averaging

(4.19) over the fading coefficient I, i.e.

$$P_{av} = \int_0^{+\infty} P(I) f_I(I) dI = \int_0^{+\infty} Q\left(\frac{\eta I}{\sqrt{2N_0}}\right) f_I(I) dI = f_I(I)\left[\frac{1}{2} erfc\left(\frac{\eta I}{2\sqrt{N_0}}\right)\right] dI \tag{4.20}$$

The above integral can be expressed by the second kind of, v_{th} order modified Bessel function, $K_v(.)$ and complimentary error function $erfc(.)$ as Meijer G-functions $\big(erfc(\sqrt{x}) = \frac{1}{\sqrt{\pi}} G_{1\,3}^{2\,0}\left(\begin{smallmatrix} 1 \\ 0,\frac{1}{2} \end{smallmatrix}\middle| x\right)$ [34]$\big)$. Thus, (4.20) can be expressed as

$$P_{av} = \frac{2^{\alpha-2}}{\sqrt{\pi^3}\Gamma(\alpha)} G_{5\,2}^{2\,4}\left(\begin{smallmatrix} \frac{1-\alpha}{2}, \frac{2-\alpha}{2}, 0, \frac{1}{2}, 1 \\ 0, \frac{1}{2} \end{smallmatrix}\middle| \frac{4\eta^2}{N_0\alpha^2}\right) \tag{4.21}$$

In terms of the average electrical SNR of the SISO system, μ, (4.21) can be written as

$$P_{av} = \frac{2^{\alpha-2}}{\sqrt{\pi^3}\Gamma(\alpha)} G_{5\,2}^{2\,4}\left(\begin{smallmatrix} \frac{1-\alpha}{2}, \frac{2-\alpha}{2}, 0, \frac{1}{2}, 1 \\ 0, \frac{1}{2} \end{smallmatrix}\middle| \frac{4\mu}{\alpha^2}\right) \tag{4.22}$$

The numerical result of (4.22) is shown in Fig. 4.3.

If wavelength diversity to be used, its average BER will be derived by considering the channel model presented below, i.e. one transmitter and W receivers, which is clearly comparable to a single input multiple output (SIMO) case of optical communication system.

In this case, the optimum decision metric for OOK will be given by, [25]:

$$P(\overrightarrow{y} \mid off, I_w) \lesseqgtr P(\overrightarrow{y} \mid on, I_w) \tag{4.23}$$

where $\overrightarrow{y} = (y_1, y_2, ..., y_W)$ is the vector signal with W components arriving at the receivers of the wavelength diversity FSO system.

In this respect, I have derived the expressions for the average bit error rate for wavelength diversity FSO system with W different channels by using Optimal Combining (OC), Equal Gain Combining (EGC) and Selection Combining (SC) method at the receiver end.

4.5.1 Optimal Combining (OC)

The average BER of the FSO system with the W different wavelength channels, will be achieved below in the form according to [25]

$$P_W^{OC} = \int_{\overrightarrow{I}} f_{\overrightarrow{I}}(\overrightarrow{I}) Q\left(\frac{1}{\sqrt{2WN_0}} \sqrt{\sum_{w=1}^{W} (\eta_w I_w)^2} \right) d\overrightarrow{I} \tag{4.24}$$

where $\overrightarrow{I} = (I_1, I_2, ..., I_W)$ is the vector of the normalized irradiances for each of the W receivers. To integrate this integral expression, we use an approximation for the Q-function presented in [31, eq. (14)] i.e. $Q(x) \approx \frac{1}{12} exp\left(\frac{-x^2}{2}\right) + \frac{1}{4} exp\left(\frac{-2x^2}{3}\right)$ and substitute it into (4.24), now (4.24) becomes

$$P_W^{OC} \approx \frac{1}{12} \prod_{w=1}^{W} \int_0^\infty f_{I_w}(I_w) exp\left(\frac{-(\eta_w I_w)^2}{4WN_0}\right) + \frac{1}{4} \prod_{w=1}^{W} \int_0^\infty f_{I_w}(I_w) exp\left(\frac{-(\eta_w I_w)^2}{3WN_0}\right) \tag{4.25}$$

Then, by expressing the exponential function, $e^{-x} = G^{1\,0}_{0\,1}\left({}^{-}_{0} \middle| x \right)$ and the modified Bessel functions with the Meijer G-function presented in [29] and integrating, the following closed form mathematical expression will be obtained:

$$\begin{aligned} P_W^{OC} \approx & \frac{1}{12} \prod_{w=1}^{W} \left[\frac{2^{\alpha_w - 1}}{\pi \Gamma(\alpha_w)} G^{1\,4}_{4\,1} \left({}^{\frac{1-\alpha_w}{2}, \frac{2-\alpha_w}{2}, 0, \frac{1}{2}}_{0} \middle| \frac{4\eta_w^2}{\alpha_w^2 W N_0} \right) \right] \\ & + \frac{1}{4} \prod_{w=1}^{W} \left[\frac{2^{\alpha_w - 1}}{\pi \Gamma(\alpha_w)} G^{1\,4}_{4\,1} \left({}^{\frac{1-\alpha_w}{2}, \frac{2-\alpha_w}{2}, 0, \frac{1}{2}}_{0} \middle| \frac{16\eta_w^2}{3\alpha_w^2 W N_0} \right) \right] \end{aligned} \tag{4.26}$$

In terms of the average electrical SNR, (4.26) can be rewritten also as:

$$P_W^{OC} \approx \frac{1}{12}\prod_{w=1}^{W}\left[\frac{2^{\alpha_w-1}}{\pi\Gamma(\alpha_w)}G_{4\,1}^{1\,4}\left(\left.\begin{matrix}\frac{1-\alpha_w}{2},\frac{2-\alpha_w}{2},0,\frac{1}{2}\\0\end{matrix}\right|\frac{4\mu_w}{\alpha_w^2 W}\right)\right] + \frac{1}{4}\prod_{w=1}^{W}\left[\frac{2^{\alpha_w-1}}{\pi\Gamma(\alpha_w)}G_{4\,1}^{1\,4}\left(\left.\begin{matrix}\frac{1-\alpha_w}{2},\frac{2-\alpha_w}{2},0,\frac{1}{2}\\0\end{matrix}\right|\frac{16\mu_w}{3\alpha_w^2 W}\right)\right] \tag{4.27}$$

where α_w defines the w_{th} channel parameter and μ_w is the average electrical SNR of the w_{th} diversity aperture. The numerical result of (4.27) is shown in Fig. 4.4.

4.5.2 Equal Gain Combining (EGC)

The EGC method is similar to OC with an exception to neglect the weighting circuits. The average BER of the FSO system with W different channel for the case of EGC can be expressed as:

$$P_W^{EGC} = \int_{\overrightarrow{I}} f_{\overrightarrow{I}}(\overrightarrow{I})Q\left(\frac{\prod_{w=1}^{W}\eta_w I_w}{W\sqrt{2N_0}}\right)d\overrightarrow{I} \tag{4.28}$$

Following the calculation procedure of the OC method, the final average BER expression for EGC can be expressed as:

$$P_W^{EGC} \approx \frac{1}{12}\prod_{w=1}^{W}\left[\frac{2^{\alpha_w-1}}{\pi\Gamma(\alpha_w)}G_{4\,1}^{1\,4}\left(\left.\begin{matrix}\frac{1-\alpha_w}{2},\frac{2-\alpha_w}{2},0,\frac{1}{2}\\0\end{matrix}\right|\frac{4\mu_w}{\alpha_w^2 W^2}\right)\right] + \frac{1}{4}\prod_{w=1}^{W}\left[\frac{2^{\alpha_w-1}}{\pi\Gamma(\alpha_w)}G_{4\,1}^{1\,4}\left(\left.\begin{matrix}\frac{1-\alpha_w}{2},\frac{2-\alpha_w}{2},0,\frac{1}{2}\\0\end{matrix}\right|\frac{16\mu_w}{3\alpha_w^2 W^2}\right)\right] \tag{4.29}$$

The numerical result of (4.29) is shown in Fig. 4.5.

4.5.3 Selection Combining (SC)

The general form of selection combining is to monitor all the diversity branches and select the one which has the highest SNR. Therefore, the selection of irradiance and average electrical SNR are made according to

$$I_{SC} = max(I_1, I_2, ..., I_w) \tag{4.30}$$

$$\mu_{SC} = max(\mu_1, \mu_2, ..., \mu_w) \tag{4.31}$$

The average BER of the FSO system for the case of SC can be obtained as:

$$P_W^{SC} = \int_0^\infty f_{I_{SC}}(I_{SC}) Q\left(\frac{\eta_{SC} I_{SC}}{\sqrt{2W N_0}}\right) dI_{SC} \tag{4.32}$$

where $f_{I_{SC}}(I_{SC})$ is the pdf of the maximum irradiance. For W wavelength channel the final average BER equation in terms of μ_{SC} can be expressed as

$$\begin{aligned} P_W^{SC} \approx \frac{1}{12} \prod_{w=1}^{W} \left[\frac{2^{\alpha_w - 1}}{\pi \Gamma(\alpha_w)} G^{1\,4}_{4\,1} \left({}^{\frac{1-\alpha_w}{2}, \frac{2-\alpha_w}{2}, 0, \frac{1}{2}}_{0} \middle| \frac{4\mu_{SC}}{\alpha_w^2 W} \right) \right] \\ + \frac{1}{4} \prod_{w=1}^{W} \left[\frac{2^{\alpha_w - 1}}{\pi \Gamma(\alpha_w)} G^{1\,4}_{4\,1} \left({}^{\frac{1-\alpha_w}{2}, \frac{2-\alpha_w}{2}, 0, \frac{1}{2}}_{0} \middle| \frac{16\mu_{SC}}{3\alpha_w^2 W} \right) \right] \end{aligned} \tag{4.33}$$

where μ_{SC} is the maximum average SNR achieved by the system for the irradiance I_{SC}.

The numerical result of (4.33) is shown in Fig. 4.6.

We consider the propagation link length, $L_1 = 2km$ and $L_2 = 3km$, receiver aperture diameter, $D = 0.01m$ and assume three wavelengths $\lambda_1 = 1550nm, \lambda_2 = 1310nm$ and $\lambda_3 = 850nm$ for the strong atmospheric turbulence scenario. For strong turbulence refractive index structure parameter $C_n^2 = 2 \times 10^{-13} m^{\frac{-2}{3}}$ is chosen. And also assume that the average electrical SNR and the sensitivity limits are the same for all the W receivers, i.e., $\mu_1 = \mu_2 = ... = \mu_W = \mu$ and $\gamma_{th,1} = \gamma_{th,2} = ... = \gamma_{th,W} = \gamma_{th}$.

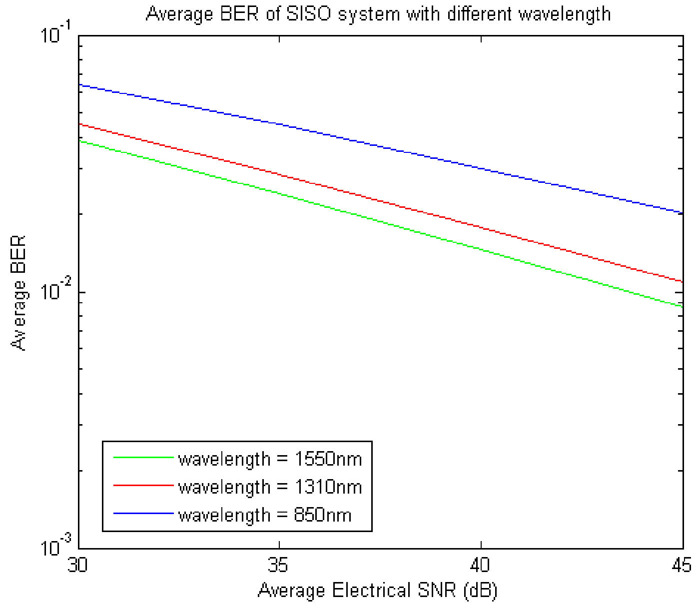

Figure 4.3: Average BER of SISO system for different operational wavelength.

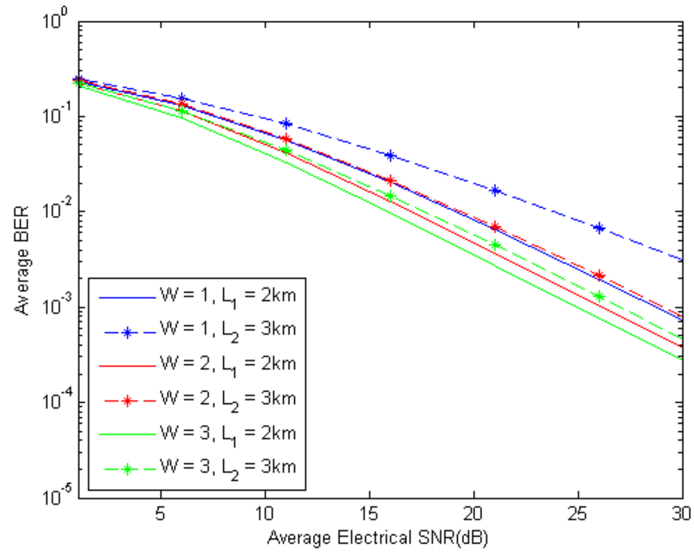

Figure 4.4: Average BER vs. Average Electrical SNR under optimal combining.

In Fig. 4.3, the average BER versus average SNR results for SISO system is shown for different operational wavelength by using (4.22). Here, we individually examine the BER performance of the system for each different wavelength channel for single transceiver system. It is clearly depicted from this figure that link operation at higher wavelength provides much better results than the operation at lower wavelengths in terms of BER. We also observe that even for high values of average SNR (i.e., 30-45 dB) the single wavelength channel fails to achieve the acceptable BER for practical FSO system. This fully justifies the use of wavelength diversity.

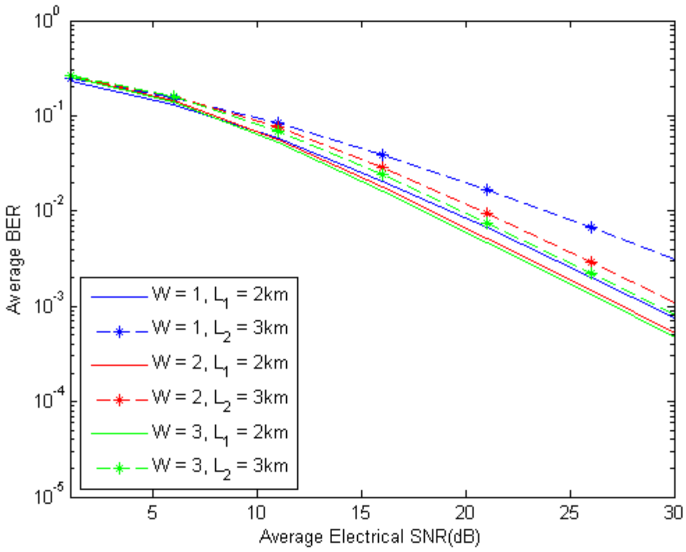

Figure 4.5: Average BER vs. Average Electrical SNR under Equal Gain combining.

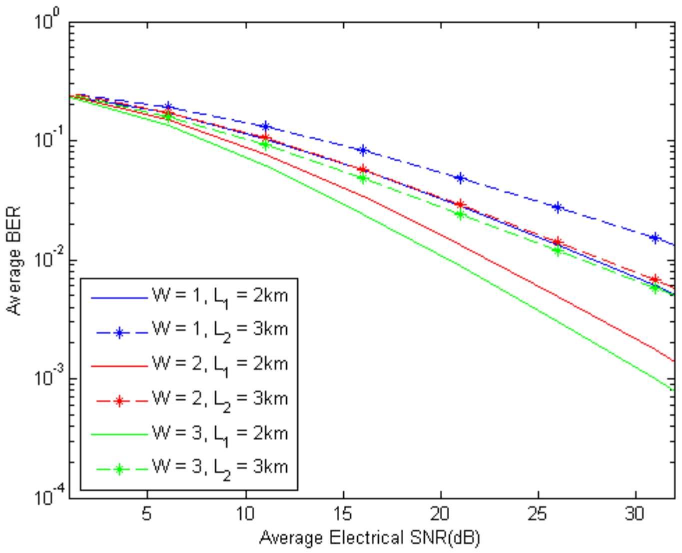

Figure 4.6: Average BER vs. Average Electrical SNR under Selection combining.

In Fig. 4.4, Fig. 4.5 and Fig. 4.6 the average BER versus average SNR results is shown by using OC in (4.27), EGC in (4.29) and SC in (4.33), respectively with $W = 1$, 2 and 3 wavelength channels. From these figures, it is clearly illustrated that the average BER is significantly improved as the number of elements (W) increases in the propagation path. For the case of $W = 3$ and $L = 2$ km the required average SNR to achieve an bit error rate of 10^{-3} for OC, EGE and SC method are 24.9 dB, 26.8 dB and 30.4 dB respectively.

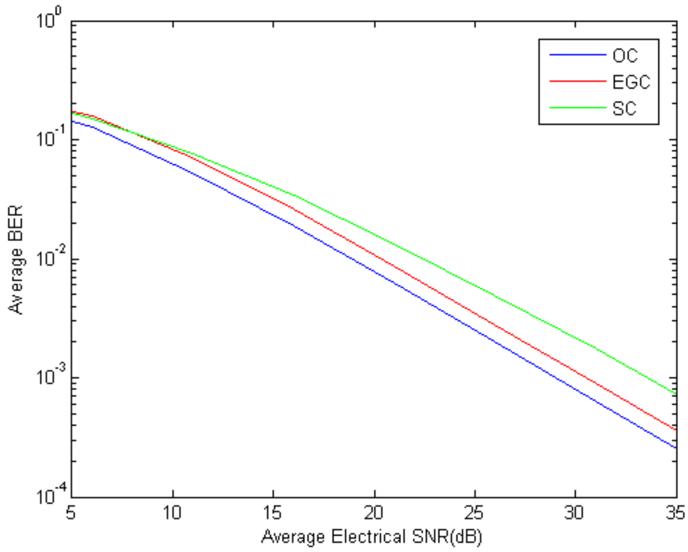

Figure 4.7: Comparison of the Average BER with OC, EGC and SC receivers of the FSO link for W = 2.

In Fig. 4.7, the Average BER vs. Average Electrical SNR with OC, EGC and SC receivers of the FSO link for $W = 2$ is demonstrated. It shows that the performance of EGC receivers is almost similar to OC receivers. The observed difference is only a 1.6 dB. From this result, it is clear that the performace obtained by OC and EGC better than SC ones.

Chapter 5

Exponentiated Weibull Channel Model with Wavelength Diversity

5.1 Introduction

The major difficulty for FSO system is to find a single distribution to model the PDF of the irradiance fluctuations, valid in all turbulence condition and under all aperture averaging conditions. The Log-Normal model is valid in weak turbulence situation for a point receiver and works well in all regimes of turbulence for aperture averaged data [32, 33] and the Gamma-Gamma model is valid in all turbulence regimes for a point receiver, but, the Gamma-Gamma model does not hold when aperture averaging takes place [33, 34]. The Exponentiated Weibull distribution offers an excellent fit to simulation and experimental data under all aperture averaging conditions, under weak and moderate turbulence conditions, as well as for point-like apertures.

In this chapter, I have considered the FSO system with wavelength diversity over Exponentiated Weibull Channel Model and evaluate their reliability and performance by the achieved outage probability and average BER for low and strong turbulence scenario in the presence of aperture averaging.

5.2 Exponentiated Weibull Channel Model

The Exponentiated Weibull (EW) distribution was first introduced by Mudholkar & Srivastava [35] as a generalization of the Weibull distribution, with the addition of an extra shape parameter. The Weibull distribution initially appearing in the field of reliability engineering [36]-has been widely used in physics and engineering to model the wind speed distribution [37], a specific type of clutter [38], and, in wireless communications where some channels are modeled with Weibull fading [39, 40].

Models in which the fading is characterized by a single PDF are only valid for stationary conditions, where the statistics of the channel are somehow invariant over the observation time period. Conversely, if the process of interest is non-stationary and the signal statistics vary significantly over the interval of interest, a mixture of model is better suited, where a weighted summation of several statistical distributions can be used [41].

The PDF of Weibull distribution is [41]:

$$f_I(I) = \frac{\beta}{\eta}\left(\frac{I}{\eta}\right)^{\beta-1} exp\left[-\left(\frac{I}{\eta}\right)^{\beta}\right] \tag{5.1}$$

where $\beta > 0$ is a shape parameter, and $\eta > 0$ is a scale parameter, that depends on β, and is related to the mean value of the irradiance. For the special cases of $\beta = 2$ and $\beta = 1$, (5.1) reduces to the Rayleigh and negative exponential PDF, respectively.

The CDF of Weibull distribution is defined by:

$$F_I(I) = 1 - exp\left[-\left(\frac{I}{\eta}\right)^{\beta}\right] \tag{5.2}$$

Assume an optical wave transmitting in the turbulent atmosphere, with multiple scatterers and random refractive-index variations. As the wave travels through this medium, multipath scattering components start to appear and cause irradiance random fluctuations of the signal-carrying laser beam. Then, the detected field at the receiver is, thus, collected by an on-axis component and a weak multipath term, composed by scattered components via different independent off-axis paths. The physical reason for this partition of the received optical field is supported by the high directivity characteristic to laser beams sources.

Considering the above justification, the irradiance I is assumed to be a weighted summation of numerous mutually independent irradiance random variables. To provide the required degrees of freedom to the mathematical model to account for uncorrelated terms a generalized average is used as follows [41]

$$I^p = \sum_{j=1}^{m} w_j I_j^p \tag{5.3}$$

where I_j are weibull random variables, and w_j are weighting factors accounting for the mean attenuation of each path. This factors are normalized such that $\sum w_j = 1$. The on-axis component is denoted by I_1, and there are $m-1$ off-axis terms. Furthermore, instead of a summation of linear components it is assumed the existence of a nonlinear relationship - as in the Weibull fading model - demonstrated in terms of a power parameter $p > 0$.

Then, in order to approximate such summation to the on-axis component, but still considering the off-axis terms the maximum function can be introduced as [41]

$$I = \lim_{p\to\infty} \left[\sum_{j=1}^{m} w_j I_j^p \right]^{\frac{1}{p}} = max\{I_1, I_2, ..., I_m\} \tag{5.4}$$

where $I_1, I_2, ..., I_m$ are independent and identically distributed weibull random variables of the irradiance data terms. Therefore, the cumulative distribution function of I_j is given by (5.2), and using the property of ordered statistics for the maximum of a sample the CDF of the irradiance is $F_I(I) = [F_{I_j}(I)]^m$. These types of distributions are referred as exponentiated distributions, were m is a non-negative integer number. Furthermore, it is a natural assumption to define $\alpha > 0$ as the real valued extension of m. The parameter α can be interpreted as the average number of on-axis and off-axis components. The α parameter should be low for weak turbulence, as there are few scatterers decreasing the probability of off-axis components to appear, increasing to a maximum value somewhere in the moderate turbulence regime, as the number of scatterers increases too. Moreover, the value of α can be lower than unity denoting deep fading events, during the observation time period, meaning that on average even the on-axis component could not reach the receiver.

Then, the PDF of a random variable I defined by the Exponentiated Weibull (EW) distribution are given by [41]

$$f_I(I) = \frac{\alpha\beta}{\eta}\left(\frac{I}{\eta}\right)^{\beta-1} exp\left[-\left(\frac{I}{\eta}\right)^{\beta}\right]\left\{1 - exp\left[-\left(\frac{I}{\eta}\right)^{\beta}\right]\right\}^{\alpha-1} \tag{5.5}$$

And the corresponding CDF is

$$F_I(I) = \left\{1 - exp\left[-\left(\frac{I}{\eta}\right)^{\beta}\right]\right\}^{\alpha} \tag{5.6}$$

where $\beta > 0$ and $\alpha > 0$ are shape parameters, and $\eta > 0$ is a scale parameter, which is related to the mean value of the irradiance. It is worth mentioning that the PDF of EW distribution includes other distributions, such as the Weibull ($\alpha = 1$), Rayleigh ($\alpha = 1, \beta = 2$), and the negative exponential ($\alpha = 1, \beta = 1$).

The n^{th} irradiance moment of the exponentiated Weibull PDF is given by [41]

$$\langle I^n \rangle = \alpha \eta^n \Gamma\left(1 + \frac{n}{\beta}\right) g_n(\alpha, \beta) \tag{5.7}$$

where $g_n(\alpha, \beta)$ was introduced to simplify the notation, and is defined by

$$g_n(\alpha, \beta) = \sum_{j=o}^{\infty} \frac{(-1)^j \Gamma(\alpha)}{j!(j+1)^{1+\frac{n}{\beta}} \Gamma(\alpha - j)} \tag{5.8}$$

The shape parameter β was found to be [41]

$$\beta \simeq 1.012(\alpha \sigma_I^2)^{\frac{-13}{25}} + 0.142 \tag{5.9}$$

And the second shape parameter α is [41]

$$\alpha \simeq 3.931\left(\frac{D}{\rho_0}\right)^{-0.519} \tag{5.10}$$

where $\rho_0 = (1.46 C_n^2 k^2 L)^{\frac{-3}{5}}$ is the atmospheric coherence radius and D is the receiver aperture diameter.

Now, it is assumed that $\langle I \rangle = 1$, and setting $n = 1$ in (5.7), then the scale parameter η is

$$\eta = \frac{1}{\alpha \Gamma\left(1 + \frac{1}{\beta}\right) g_1(\alpha, \beta)} \tag{5.11}$$

5.3 FSO system with Wavelength Diversity

Suppose that an FSO system comprises of W different pair of transmitter and receivers and the information signal is pass on all together by the W transmitters at W different wavelengths. Then, each w^{th} of these copies of the signal, $w = 1, ..., W$, will be detected only by w^{th} receiver. For a few kilometers link distances and aperture separation of the photo detectors is of order of centimeters, these W receivers will be practically uncorrelated [28]. We consider the w^{th} laser beam as it propagates along a horizontal path through turbulence channel with additive white Gaussian noise (AWGN). The channel is assumed to be memory less and ergodic, with independent and identically distributed (i.i.d.) intensity fast fading statistics, intensity modulation/direct detection (IM/DD) with On-Off Keying (OOK) modulation. In this case, the statistical channel model can be considered as [25]:

$$y_w = h_w x + n = \delta_w x I_w + n, w = 1, ..., W \tag{5.12}$$

where y_w is the output signal of each of the W receivers, $h_w = \delta_w I_w$ is instantaneous intensity gain, η_w is effective photo current conversion ratio of each receiver, I_w is the normalized irradiance arrived in each receiver and x is the modulated signal with binary values '0' or '1', and n represents the AWGN with zero mean and variance equal to $\frac{N_0}{2}$.

After applying Wavelength diversity over EW distribution, the PDF of the distribution is given by:

$$f_{I_w}(I_w) = \frac{\alpha_w \beta_w}{\eta_w}\left(\frac{I_w}{\eta_w}\right)^{\beta_w - 1} exp\left[-\left(\frac{I_w}{\eta_w}\right)^{\beta_w}\right]\left\{1 - exp\left[-\left(\frac{I_w}{\eta_w}\right)^{\beta_w}\right]\right\}^{\alpha_w - 1} \tag{5.13}$$

And the corresponding CDF is

$$F_{I_w}(I_w) = \int_0^\infty f_{I_w}(I_w) dI_w \tag{5.14}$$

or,

$$F_{I_w}(I_w) = \left\{1 - exp\left[-\left(\frac{I_w}{\eta_w}\right)^{\beta_w}\right]\right\}^{\alpha_w} \tag{5.15}$$

where $\beta_w > 0$ and $\alpha_w > 0$ are two shape parameters related to the scintillation index, and $\eta_w > 0$ is a scale parameter, which is related to the mean value of the irradiance I_w for w_{th} wavelength channel. The extra shape parameter, α_w gives more versatility to the EW distribution in the shape of the tails [49]. For fixed values of the shape parameter β_w and the scale parameter η_w, the shape parameter α_w controls the lower-tail steepness when data is visualized in a logarithmic scale. This is an attractive property of the EW distribution; it is precisely the lower-tail of maximum importance because it defines the error rate and fades probability [42].

The expression for the shape parameter α_w for w_{th} wavelength is given by;

$$\alpha_w \simeq 3.931\left(\frac{D}{\rho_{0,w}}\right)^{-0.519} \tag{5.16}$$

where D is the receiving aperture diameter and $\rho_{0,w}$ is the atmospheric coherence radius with w_{th} wavelength which is given by

$$\rho_{0,w} = (1.46C_n^2 k_w^2 L)^{\frac{-3}{5}} \tag{5.17}$$

Here $k_w = \frac{2\pi}{\lambda_w}$, is the wave number, λ_w is the operational wavelength of each of the W channels of the FSO system and L is the distance between the transmitter and receiver planes. The C_n^2 represents the refractive index structure parameter, depends on the altitude and the atmospheric conditions [42].

The shape parameter β_w is related to the scintillation index, σ_I^2 as;

$$\beta_w \simeq 1.012(\alpha_w \sigma_{I_w}^2)^{\frac{-13}{25}} + 0.142 \tag{5.18}$$

And the scale parameter η_w is given by

$$\eta_w = \frac{1}{\alpha_w \Gamma\left(1 + \frac{1}{\beta_w}\right) g_1(\alpha_w, \beta_w)} \tag{5.19}$$

where $g_1(\alpha_w, \beta_w)$ with w_{th} wavelength is calculated by

$$g_1(\alpha_w, \beta_w) = \sum_{j=o}^{\infty} \frac{(-1)^j \Gamma(\alpha_w)}{j!(j+1)^{1+\frac{1}{\beta_w}} \Gamma(\alpha_w - j)} \tag{5.20}$$

For w_{th} wavelength, the instantaneous electrical SNR can be defined as $\gamma_w = \frac{(\delta_w I_w)^2}{N_0}$ and the average electrical SNR is defined as, $\mu_w = \frac{(\delta_w E[I_w])^2}{N_0}$. Here, $E[I_w] = 1$ since I_w is normalized. After a power transformation of the random variable I_w, the PDF of the instantaneous electrical SNR,γ_w with w_{th} wavelength can be derived as,

$$f_{\gamma_w}(\gamma_w) = \frac{\alpha_w \beta_w}{\eta_w} exp\left[-\left(\frac{1}{\eta_w}\sqrt{\frac{\gamma_w}{\mu_w}}\right)^{\beta_w}\right] \left\{1 - exp\left[-\left(\frac{1}{\eta_w}\sqrt{\frac{\gamma_w}{\mu_w}}\right)^{\beta_w}\right]\right\}^{\alpha_w - 1} \tag{5.21}$$

And the corresponding CDF of the instantaneous electrical SNR γ_w is;

$$F_{\gamma_w}(\gamma_w) = \left\{1 - exp\left[-\left(\frac{1}{\eta_w}\sqrt{\frac{\gamma_w}{\mu_w}}\right)^{\beta_w}\right]\right\}^{\alpha_w} \tag{5.22}$$

Thus, from mathematical expressions (5.21) and (5.22) it is clear that both PDF and CDF of the instantaneous electrical SNR of EW channel strongly depends on the atmospheric conditions.

5.4 The Outage Probability

The outage probability represents the probability that the instantaneous SNR falls below the critical threshold, γ_{th} which corresponds to the receiver's input sensitivity limit. Using the above expression, (5.22), for the EW channel CDF, closed form expressions for the outage probability of the FSO system with wavelength diversity is derived by optimal combining (OC).

The outage probability, P_out of the FSO system for single channel ($i.e., W = 1$) is given by

$$P_{out} = P_r(\gamma \leq \gamma_{th}) = F_\gamma(\gamma_{th}) \tag{5.23}$$

And using (5.22):

$$P_{out} = \left\{1 - exp\left[-\left(\frac{1}{\eta}\sqrt{\frac{\gamma_{th}}{\mu}}\right)^{\beta}\right]\right\}^{\alpha} \tag{5.24}$$

The numerical result of (5.24) is shown in Fig. 5.1 for different threshold SNR.

For multiple wavelength channel, W, assuming that the outage Probability is independent for each one of the W channels, then the total outage probability $P_{out,W}$ of the considered FSO systems will correspond to the probability of outage of all the W links, i.e.,

$$P_{out,W} = \prod_{w=1}^{W} P_{out,w} = \prod_{w=1}^{W} P_r(\gamma_w \leq \gamma_{th,w}) = \prod_{w=1}^{W} F_{\gamma_w}(\gamma_{th,w}) \tag{5.25}$$

or,

$$P_{out,W} = \prod_{w=1}^{W}\left[\left\{1 - exp\left[-\left(\frac{1}{\eta_w}\sqrt{\frac{\gamma_{th,w}}{\mu_w}}\right)^{\beta_w}\right]\right\}^{\alpha_w}\right] \tag{5.26}$$

The numerical result of (5.26) is shown in Fig. 5.2 and Fig. 5.3 for link length 1.5 km and 2.5 km respectively.

5.5 The Average BER of the System

The average bit error rate is an important metric for the reliability of a communication system. For the considered FSO system with IM/DD and OOK, the estimation, of BER, P_e, in the presence of AWGN can be done through the expression:

$$P_e = P(1)P(e \mid 1) + P(0)P(e \mid 0) \tag{5.27}$$

where $P(1)$ and $P(0)$ are the probabilities of sending 1 and 0 bits, respectively, and $P(e \mid 1)$ and $P(e \mid 0)$ represent the conditional bit error probabilities when the transmitted bit is 1 and 0. Then assuming that the condition is symmetric, i.e. $P(1) = P(0) = 0.5$, and $P(e \mid 1) = P(e \mid 0)$, the estimation of BER for SISO link (Assuming the case $W = 1$), as a function of I, is given as:

$$P_e(I) = P(e \mid 1, I) + P(e \mid 0, I) = Q\left(\frac{\delta I}{\sqrt{2N_0}}\right) = Q\left(\sqrt{\frac{\gamma}{2}}\right) \tag{5.28}$$

where $Q(.)$ is the Gaussian Q-function defined as $Q(x) = \left(\frac{1}{\sqrt{2N_0}}\right)\int_x^{\infty} exp\left(\frac{t^2}{2}\right)dt$ and this is also related to the complimentary error function $erfc(.)$ by $erfc(x) = 2Q(\sqrt{2}x)$.

The average BER of EW channel for SISO link of the FSO system, P_{av} is obtained by averaging (5.28) over the fading coefficient I, i.e.

$$P_{av} = \int_0^{+\infty} P_e(I) f_I(I) dI = \int_0^{+\infty} Q\left(\frac{\delta I}{\sqrt{2N_0}}\right) f_I(I) dI \tag{5.29}$$

In this case we will compute average BER from the CDF, $F_I(I)$, as follows

$$P_{av} = -\int_0^{+\infty} P_e^{'}(I) F_I(I) dI \tag{5.30}$$

where $P_e^{'}(I)$ is the first order derivative of the conditional BER $P_e(I)$. Now,

$$P_e^{'}(I) = -\frac{1}{\sqrt{\pi}} exp\left(\frac{-\delta^2 I^2}{4N_0}\right) = -\frac{1}{\sqrt{\pi}} exp\left(\frac{-\gamma}{4}\right) \tag{5.31}$$

Substituting (5.15) and (5.31) into (5.30), we get

$$P_{av} = \frac{1}{\sqrt{\pi}} \int_0^{+\infty} exp\left(\frac{-\delta^2 I^2}{4N_0}\right) = -\frac{1}{\sqrt{\pi}} exp\left(\frac{-\gamma}{4}\right)\left\{1 - exp\left[-\left(\frac{I}{\eta}\right)^{\beta}\right]\right\}^{\alpha} dI \tag{5.32}$$

Unfortunately, no closed-form solution for the integral (5.32) appears to be available. On the other hand, if we perform the variable $x^2 = \frac{\delta^2 I^2}{4N_0} = \frac{\sqrt{\gamma}}{2}$, (5.32) becomes

$$P_{av} = \frac{2\sqrt{N_0}}{\delta\sqrt{\pi}} \int_{-\infty}^{+\infty} exp(-x^2)\left\{1 - exp\left[-\left(\frac{2\sqrt{N_0}}{\delta\eta}x\right)^{\beta}\right]\right\}^{\alpha} dI \tag{5.33}$$

Here (5.33) is in the form of $\int_{-\infty}^{+\infty} g(x)e^{-x^2}$, where $g(x) = \left\{1 - exp\left[-\left(\frac{2\sqrt{N_0}}{\delta\eta}x\right)^{\beta}\right]\right\}^{\alpha}$, and it can be approximated by using Gauss–Hermite quadrature rule.

The Gauss–Hermite quadrature approximation can be defined as [43];

$$\int_{-\infty}^{+\infty} g(x)e^{-x^2} \approx \sum_{i=1}^{n} w_i g(x_i) \tag{5.34}$$

where n is the number of sample point used. The x_i are the roots of the Hermite Polynomials $H_n(x)(i = 1, 2, ..., n)$ and the associated weight w_i are given by [43]

$$W_i = \frac{2^{(n-1)} n! \sqrt{\pi}}{n^2[H_{n-1}(x_i)]^2} \tag{5.35}$$

Using (5.34) and (5.35), (5.33) can be written as

$$P_{av} \approx \frac{2\sqrt{N_0}}{\delta\sqrt{\pi}} \sum_{i=1}^{n} w_i \left\{1 - exp\left[-\left(\frac{2\sqrt{N_0}}{\delta\eta}x_i\right)^{\beta}\right]\right\}^{\alpha} dI \tag{5.36}$$

In terms of the average electrical SNR of the SISO system, μ, (5.36) can be written as

$$P_{av} \approx \frac{2}{\sqrt{\pi\mu}} \sum_{i=1}^{n} w_i \left\{ 1 - exp\left[- \left(\frac{2}{\eta\sqrt{\mu}} x_i \right)^{\beta} \right] \right\}^{\alpha} dI \tag{5.37}$$

The numerical result of (5.37) is shown in Fig. 5.4 for different wavelength.

If wavelength diversity to be used, its average BER will be derived by considering the channel model presented below, i.e. one transmitter and W receivers, which is clearly comparable to a single input multiple output (SIMO) case of optical communication system.

In this case, the optimum decision metric for OOK will be given by, [25]:

$$P(\overrightarrow{y} \mid off, I_w) \lessgtr P(\overrightarrow{y} \mid on, I_w) \tag{5.38}$$

where $\overrightarrow{y} = (y_1, y_2, ..., y_W)$ is the vector signal with W components arriving at the receivers of the wavelength diversity FSO system.

In this respect, I have derived the expressions of the average bit error rate for wavelength diversity system with W different channels by using Optimal Combining (OC) method at the receiver end.

The average BER of the FSO system with the W different wavelength channels for OC system, will be achieved below in the form according to [30]:

$$P_{W,OC} = \int_{\overrightarrow{I}} f_{\overrightarrow{I}}(\overrightarrow{I}) Q\left(\frac{1}{\sqrt{2WN_0}} \sqrt{\sum_{w=1}^{W} (\eta_w I_w)^2} \right) d\overrightarrow{I} \tag{5.39}$$

where $\overrightarrow{I} = (I_1, I_2, ..., I_W)$ is the vector of the normalized irradiances for each of the W receivers.

In terms of CDF, $F_{I_w}(I_w)$, the average BER for w_{th} wavelength will be

$$P_{W,OC} = \prod_{w=1}^{W} \frac{1}{\sqrt{\pi}} \int_0^{+\infty} exp\left(\frac{-\delta_w^2 I_w^2}{4N_0}\right)\left\{1 - exp\left[-\left(\frac{I_w}{\eta_w}\right)^{\beta_w}\right]\right\}^{\alpha_w} dI_w \tag{5.40}$$

Following the calculation procedure of the SISO link, the average BER expression with wavelength diversity can be expressed as:

$$P_{W,OC} \approx \prod_{w=1}^{W} \frac{2\sqrt{WN_0}}{\delta_w\sqrt{\pi}} \sum_{i=1}^{n} w_i \left\{1 - exp\left[-\left(\frac{2\sqrt{WN_0}}{\delta_w \eta_w} x_i\right)^{\beta_w}\right]\right\}^{\alpha_w} dI \tag{5.41}$$

In the form of average electrical SNR, μ_w, the final average BER expression for OC system can be expressed as:

$$P_{W,OC} \approx \prod_{w=1}^{W} \frac{2\sqrt{W}}{\sqrt{\pi\mu_w}} \sum_{i=1}^{n} w_i \left\{1 - exp\left[-\left(\frac{2\sqrt{W}}{\eta_w\sqrt{\mu_w}} x_i\right)^{\beta_w}\right]\right\}^{\alpha_w} dI \tag{5.42}$$

where μ_w defines the average electrical SNR for the w_{th} wavelength channel.

The numerical result of (5.42) is shown in Fig. 5.5 and Fig. 5.6 for link length 1.5 km and 2.5 km respectively.

The numerical results for the outage probability and average BER of an EW channel are plotted for different system parameters that are affect the performance of the FSO system. Such parameters are the number W of the different channels, the related wavelengths for the case of wavelength diversity, $\lambda_w(w = 1, \ldots, W)$, the propagation link length L, the refractive index structure parameter, C_n^2 and the receiver aperture diameter, D. Note that the effectiveness of receiver diversity is reduced under the correlated fading conditions caused by small aperture spacing. Assuming appropriate aperture spacing (usually on the order of a few centimeters), we consider the independent channel fading for all the cases and assume $D = 60mm$ and three different wavelengths, these are: $\lambda_1 = 1.55\mu m, \lambda_2 = 1.31\mu m$, and $\lambda_3 = 0.85\mu m$. And considering the link length $L_1 = 1.5km$ and $L_2 = 2.5km$ and two different atmospheric turbulence conditions: moderate ($C_n^2 = 6 \times 10^{-14} m^{\frac{-2}{3}}$) and strong ($C_n^2 = 2 \times 10^{-13} m^{\frac{-2}{3}}$). Now, for the wavelength diversity scheme, we consider that the average electrical SNR and the sensitivity limits are the same for all the W receivers, i.e., $\mu_1 = \mu_2 = ... = \mu_W = \mu$ and $\gamma_{th,1} = \gamma_{th,2} = ... = \gamma_{th,W} = \gamma_{th}$.

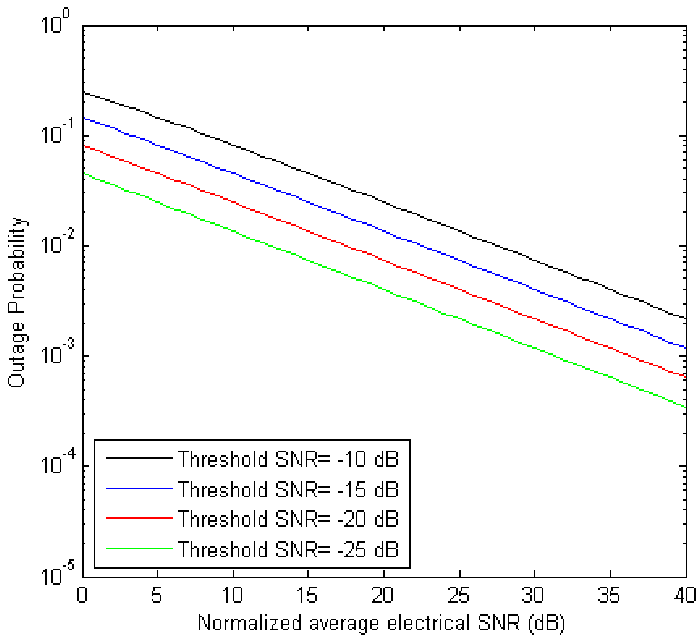

Figure 5.1: Outage probability versus Normalized average electrical SNR for different threshold SNR.

Fig. 5.1 shows the relation between outage probability and normalized average electrical SNR for different threshold values by using (5.24). From the analysis of the plots it is clear that, on different threshold SNR we get the different outage probability value but even for the high value of average SNR, we cannot achieve acceptable outage value for practical FSO systems.

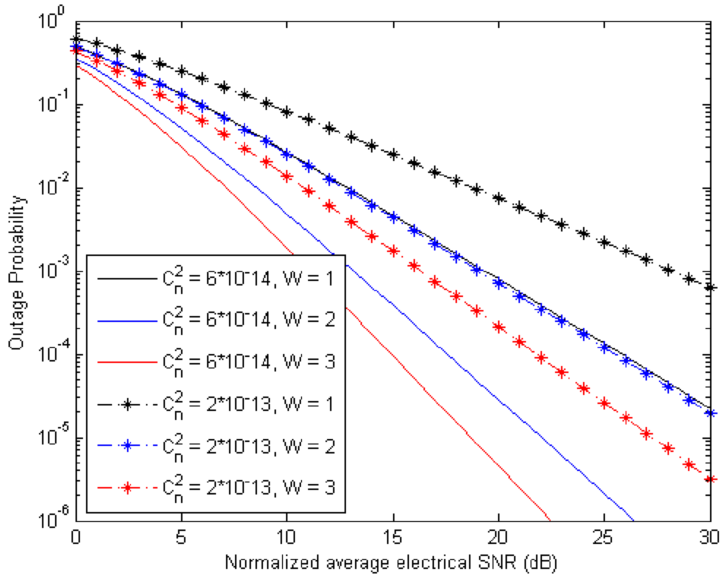

Figure 5.2: Outage probabilities versus Normalized average electrical SNR with wavelength diversity for link length of 1.5 km.

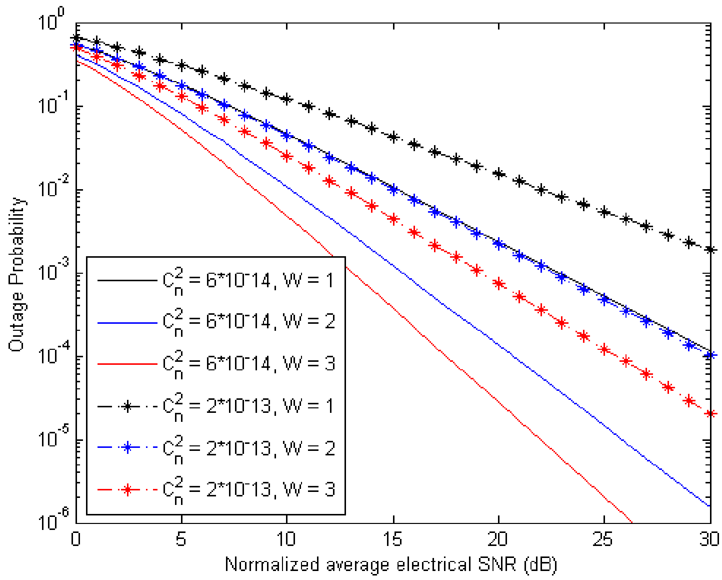

Figure 5.3: Outage probabilities versus Normalized average electrical SNR with wavelength diversity for link length of 2.5 km.

The estimation of the outage probability versus the normalized average electrical SNR of FSO links by using OC in (5.26) is shown in Fig. 5.2 and Fig. 5.3 for two different atmospheric turbulence conditions, moderate ($C_n^2 = 6 \times 10^{-14} m^{\frac{-2}{3}}$) and strong ($C_n^2 = 2 \times 10^{-13} m^{\frac{-2}{3}}$) and $W = 1, 2$ and 3 wavelength channels with propagation link length $L_1 = 1.5km$ and $L_2 = 2.5km$ respectively. From this figure it is clear that, on single threshold value the outage probability of an FSO system using wavelength diversity scheme is getting significantly smaller as the number W of different wavelength channels is increasing.

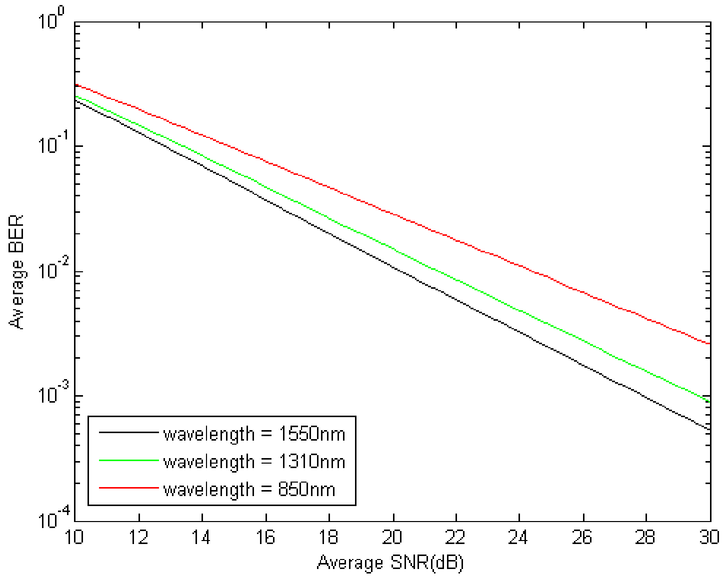

Figure 5.4: Average BER versus Average electrical SNR of SISO system for different wavelength.

In Fig. 5.4, the average BER versus average electrical SNR for different wavelength is shown by using (5.37).

It is clearly evident from this figure, as the value of the operational wavelength increases, the BER decreases but even for the high value of average SNR, BER performance for any practical systems is not very good. This fully justifies the use of wavelength diversity.

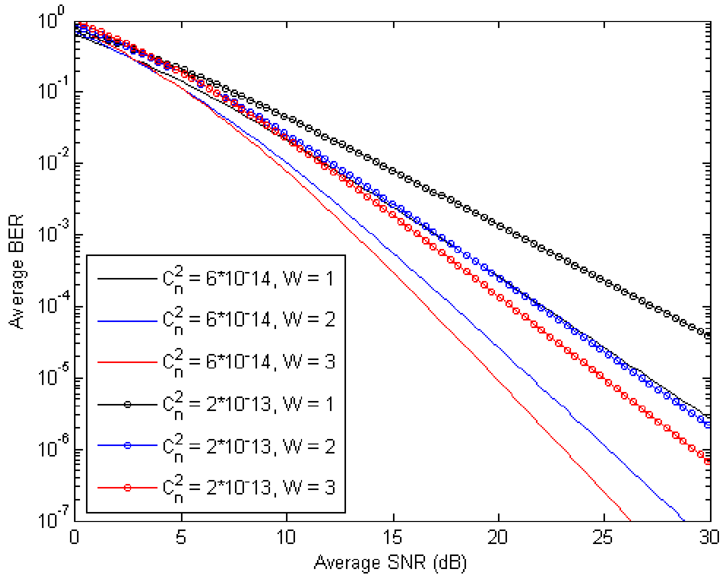

Figure 5.5: Average BER versus Average electrical SNR of FSO systems with wavelength diversity for link length of 1.5 km.

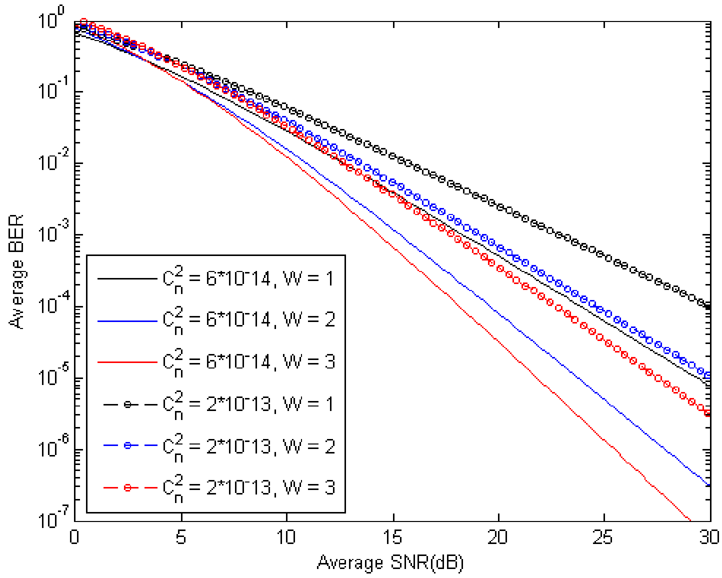

Figure 5.6: Average BER versus Average electrical SNR of FSO systems with wavelength diversity for link length of 2.5 km.

In Fig. 5.5 and Fig. 5.6, the average BER versus Average electrical SNR of FSO systems is shown with wavelength diversity by using OC in (5.42) for moderate and strong atmospheric turbulence conditions with $W = 1, 2$ and 3 wavelength channels and link length $L_1 = 1.5km$ and $L_2 = 2.5km$ respectively. From these figure, it is clearly illustrated that the average BER of FSO communication system is significantly improved as the number of elements (W) increases in the propagation path.

Chapter 6

Conclusions and Future Scope

6.1 Conclusions

The aim of this thesis is to examine the performance of free space optical systems in turbulent channels. Many statistical models have been discussed to model the random phenomena of the intensity variation over atmospheric channels. Due to the simplicity, log-normal channel model has been the most widely used model. But this model is only applicable for weak turbulence conditions. As the strength of turbulence increases, lognormal model show large deviations compared to experimental data and it disturbs the accuracy of the system performance. To overcome the limitations of the lognormal channel, other channel model have been proposed to describe atmospheric turbulence conditions. As example, the gamma-gamma and the Exponentiated Weibull channel model are suitable for weak to strong turbulence and K channel model is suitable for strong turbulence.

In this work, performance of FSO communication systems is measured in terms of BER and outage probability using wavelength diversity over K channel model and the Exponentiated Weibull channel model. I have derived mathematical expressions for the average BER and outage probability of SIMO FSO. From the presented results, it is clearly analyzed that the link operation at higher wavelength provides much better results than the operation at lower wavelengths in terms of BER but even for high values of average SNR the single wavelength channel fails to achieve the acceptable BER for FSO system. This completely justifies the use of wavelength diversity.

The results also shows that the use of wavelength diversity at the receiver improve the quality of FSO systems similar to RF ones but the system's complexity and cost increases, due to the fact that each different wavelength would truly require the operation of one more new trans-receiver.

6.2 Future Scope

While a number of key results for FSO communication have already been achieved, many more issues remain to be addressed, and many possible directions for future research exist. Throughout this dissertation, the case of wavelength diversity is considered over Log-Normal, Gamma-Gamma, K-channel and Exponentiated weibull channel model to achieve the better performance for the FSO system. It would be interesting to extend the results and examine the performance of FSO system for other fading distributions, such as Rayleigh, Ricean and Nakagami fading. In this work I have considered only On-off Keying modulation scheme, a research is also going on improving the capacity and performance of FSO systems through different type of modulation schemes, like PPM and DPSK.

Bibliography

[1] Z. Ghassemlooy and W.O. Popoola,"Terrestrial free-space optical communications", in Mobile and Wireless Communications Network Layer and Circuit Level Design, first edition, Edited by: Salma Ait Fares and Fumiyuki Adachi, Ed. India: InTech, pp. 355–392, 2010.

[2] Wasiu Oyewole Popoola,"Subcarrier intensity modulated free-space optical communication systems", Doctoral Dissertation, School of Computing, Engineering and Information Sciences, Northumbria University, Newcastle, UK, Sep. 2009.

[3] "Kablosuziletim - FSO", *Kablosuziletisim.com*, 2016. [Online]. Available: http://www.kablosuziletisim.com/fso.htm.

[4] Michael L. Baedke,"Performance analysis of multi pulse PPM on MIMO free space optical channels", Doctoral Dissertation, School of Engineering and Applied Science, University of Virginia, Virginia, USA, Aug. 2004.

[5] S. Sheikh Muhammad, Tomaz Javornik, Igor Jelovcan, Zabih Ghassemlooy, and Erich Leitgeb", Comparison of hard-decision and soft-decision channel coded M-ary PPM performance over free space optical links,"European Transactions on Telecommunications, vol. 20, no. 8, pp. 746–757, Dec. 2009.

[6] T. Pfau, S. Hoffmann, O. Adamczyk, R. Peveling, V. Herath, M. Porrmann, and R. Noé, "Coherent optical communication: towards realtime systems at 40 Gbit/s and beyond", Optics Express, vol. 16, no. 2, pp. 866-872, Jan. 2008.

[7] Z. Ghassemlooy and A R Hayes, "Indoor optical wireless communications systems – Part I: Review", School of Engineering, Northumbria University, UK, 2003.

[8] Frédéric Demers, Halim Yanikomeroglu, and Marc St-Hilaire, "A survey of opportunities for free space optics in next generation cellular networks", Proceeding of the 9th Annual Communication Networks and Service Research Conference (CNSR), Ottawa, Canada, pp. 210-216, May. 2011.

[9] Scott Bloom, Eric Korevaar, John Schuster, and Heinz Willebrand, "Understanding the performance of free-space optics", Journal of Optical Networking, vol. 2, no. 6, pp. 178-200, Jun 2003.

[10] Ivan Djordjevic, William Ryan, and Bane Vasic, "Coding for Optical Channels", Springer, New York, USA, 2010.

[11] John M. Senior,"Optical Fiber Communications Principles and Practice", Prentice Hall, Essex, England, 2009.

[12] "Channel Models: A Tutorial", *Cse.wustl.edu*, 2016. [Online]. Available: http://www.cse.wustl.edu/∼jain/wimax/channel_model_tutorial.htm.

[13] L. C. Andrews and R. L. Philips, *Laser Beam Propagation through Random Media*, 2nd ed. Belligham: SPIE Press, 2005.

[14] A. N. Kolmogorov, "The local structure of turbulence in an incompressible viscous fluid for very large reynolds numbers", *C. R. (Doki) Acad. Sci. U.S.R.R.*, vol. 30, pp. 301–305, 1941.

[15] David J. C. Dennis and timothy B. Nickels, "On the limitations of Taylor's hypothesis in constructing long structures in a turbulent boundary layer", *Journal of Fluid Mechanics*, vol. 614, pp. 197- 206, November 2008.

[16] R. S. Lawrence, G. R. Ochs, and S. F. Clifford, "Measurements of atmospheric turbulence relevant to optical propagation", *J. Opt. Soc. Am.*, vol. 60, no. 6, pp. 826–830, 1970.

[17] D. Sadot and N. S. Kopeika, "Forecasting optical turbulence strength on the basis of macroscale meteorology and aerosols: models and validation", *Opt. Eng.*, vol. 31, no. 31, pp. 200–212, 1992.

[18] Akira Ishimaru, "Wave Propagation and Scattering in Random Media", *IEEE Press and Oxford University Press*, 1997.

[19] H. T. Yura, C. C. Sung, S. F. Clifford, and R. J. Hill, "Second-order Rytov approximation", *J. Opt. Soc. Am.*, vol. 73, no. 4, pp. 500–502, 1983.

[20] R. Barrios, "Exponentiated Weibull Fading Channel Model in Free-Space Optical Communications under Atmospheric Turbulence", *Ph.D. Dissertation, Departament of Signal Theory and Comunicacions*, Polytechnic University of Catalonia, Barcelona, Spain, pp. 1-5, April, 2013.

[21] Hassan Moradi, Maryam Falahpour, Hazem H. Refai, Peter G. LoPresti, Mohammed Atiquzzaman, "BER Analysis of Optical Wireless Signals through Lognormal Fading Channels with Perfect CSI", *17th International Conference on Telecommunications*, pp. 493-497, 2010.

[22] Murat Uysal, Jing (Tiffany) Li, "Error Rate Performance of Coded Free-Space Optical Links over Gamma-Gamma Turbulence Channels", *IEEE Communications Society*, pp. 3331-3335, 2004.

[23] Neelam Srivastawa, "Diversity Schemes for Wireless Communication: A short review", *Journal of Theoretical and Applied Information Technology, Islamabad, Pakistan*, Vol.15. No.2, pp. 134-142, 31st May 2010.

[24] Pravin W. Raut, Dr. S.L. Badjate, "Diversity Techniques for Wireless Communication", *IJARET*, Vol. 4, Issue 2, March – April 2013, pp. 144-160.

[25] V. Xarcha, A. N. Stassinakis, H. E. Nistazakis, A. Tsigopoulos, "Wavelength Diversity for Free Space Optical Systems: Performance Evaluation over Lognormal Turbulence Channels", *19th International Conference on Microwaves, Radar, and Wireless Communications, Warsaw, Poland*, pp. 678-683, May 21-23, 2012.

[26] Hector E. Nistazakis, George S. Tombras, "On the use of wavelength and time diversity in optical wireless communication systems over gamma-gamma turbulence channels", *Optics & Laser Technology*, Vol. 44, pp. 2088-2094, 2012.

[27] H.G. Sandalidis and T.A. Tsiftsis "Outage probability and ergodic capacity of free-space optical links over strong turbulence", *Electronics Lett.*, Vol. 44, no. 1, pp. 46-47, 2008.

[28] Rachmani R, Arnon S., "Wavelength diversity in turbulence channels for sensor networks", *IEEE 26th Convention of Electrical and Electronics Engineers in Israel, IEEEI*, pp. 915–918, 2010.

[29] V. S. Adamchik and O. I. Marichev, "The algorithm for calculating integrals of hypergeometric type functions and its realization in REDUCE system", in *Proc. Int. Conf. on Symbolic and Algebraic Computation, Tokyo, Japan*, pp. 212-224, 1990.

[30] "The Wolfram functions site", *wolfram.com*, 2004. [Online]. Available: http://functions.wolfram.com.

[31] M. Chiani, D. Dardari, and M. K. Simon, "New exponential bounds and approximations for the computation of error probability in fading channels", *IEEE Trans. Wireless Comm.*, vol. 2, no. 4, pp. 840-845, July 2003.

[32] N. Perlot and D. Fritzsche, "Aperture-averaging – theory and measurements", in Free-Space Laser Communication Technologies XVI, ser. *Proc. SPIE*, G. Mecherle, C. Y. Young, and J. S. Stryjewski, Eds., vol. 5338, pp. 233–242, 2004.

[33] F. S. Vetelino, C. Young, and L. Andrews, "Fade statistics and aperture averaging for Gaussian beam waves in moderate-to-strong turbulence", *Appl. Opt.*, vol. 46, no. 18, pp. 3780–3790, 2007.

[34] B. Epple, "Simplified channel model for simulation of free-space optical communications", *J. Opt. Commun. Netw.*, vol. 2, no. 5, pp. 293–304, 2010.

[35] G. Mudholkar and D. Srivastava, "Exponentiated Weibull family for analyzing bathtub failure-rate data", *IEEE Trans. Reliab.*, vol. 42, no. 2, pp. 299–302, 1993.

[36] W. Weibull, "A statistical distribution function of wide applicability", *J. Appl. Mech.-Trans. ASME*, vol. 18, no. 3, p. 293297, 1951.

[37] J. V. Seguro and T. W. Lambert, "Modern estimation of the parameters of the Weibull wind speed distribution for wind energy analysis", *J Wind. Eng. Ind. Aerod.*, vol. 85, no. 1, pp. 75–84, 2000.

[38] D. Schleher, "Radar detection in Weibull clutter", *IEEE Trans. Aerosp. Electron. Syst.*, vol. AES-12, no. 6, pp. 736–743, nov. 1976.

[39] M. Lupupa and M. Dlodlo, "Performance of MIMO system in Weibull fading channel - Channel capacity analysis", *EUROCON'09*, pp. 1735 –1740, May 2009.

[40] N. C. Sagias, D. A. Zogas, G. K. Karagiannidis, and G. S. Tombras, "Channel capacity and second-order statistics in Weibull fading", *IEEE Commun. Lett.*, vol. 8, no. 6, pp. 377–379, 2004.

[41] R. Barrios and F. Dios, "Optics & Laser Technology Exponentiated Weibull model for the irradiance probability density function of a laser beam propagating through atmospheric turbulence", *Opt. Laser Technol.*, vol. 45, pp. 13–20, 2013.

[42] D. Datta and D. Datta, "Comparison of Weibull Distribution and Exponentiated Weibull Distribution Based Estimation of Mean and Variance of Wind Data", *Int. J. Energy, Inf. Commun.*, vol. 4, no. 4, pp. 1-12, 2013.

[43] Abramowitz, M & Stegun, I A, *Handbook of Mathematical Functions*, 10th printing with corrections, Dover, ISBN 978-0-486-61272-0. Equation 25.4.46, 1972.

Publications based on the Thesis

1. Bindiya Mishra, Dhaval Shah and D. K. Kothari, "Performance of Free Space Optical Link using Wavelength Diversity over K Turbulence Channels", presented in 5^{th} *IEEE International Conference on Communication and Signal Processing-ICCSP'16*.